Particle Detectors for Colliders

Semiconductor Tracking Detectors

Robert S. Orr
University of Toronto

Generic Detector

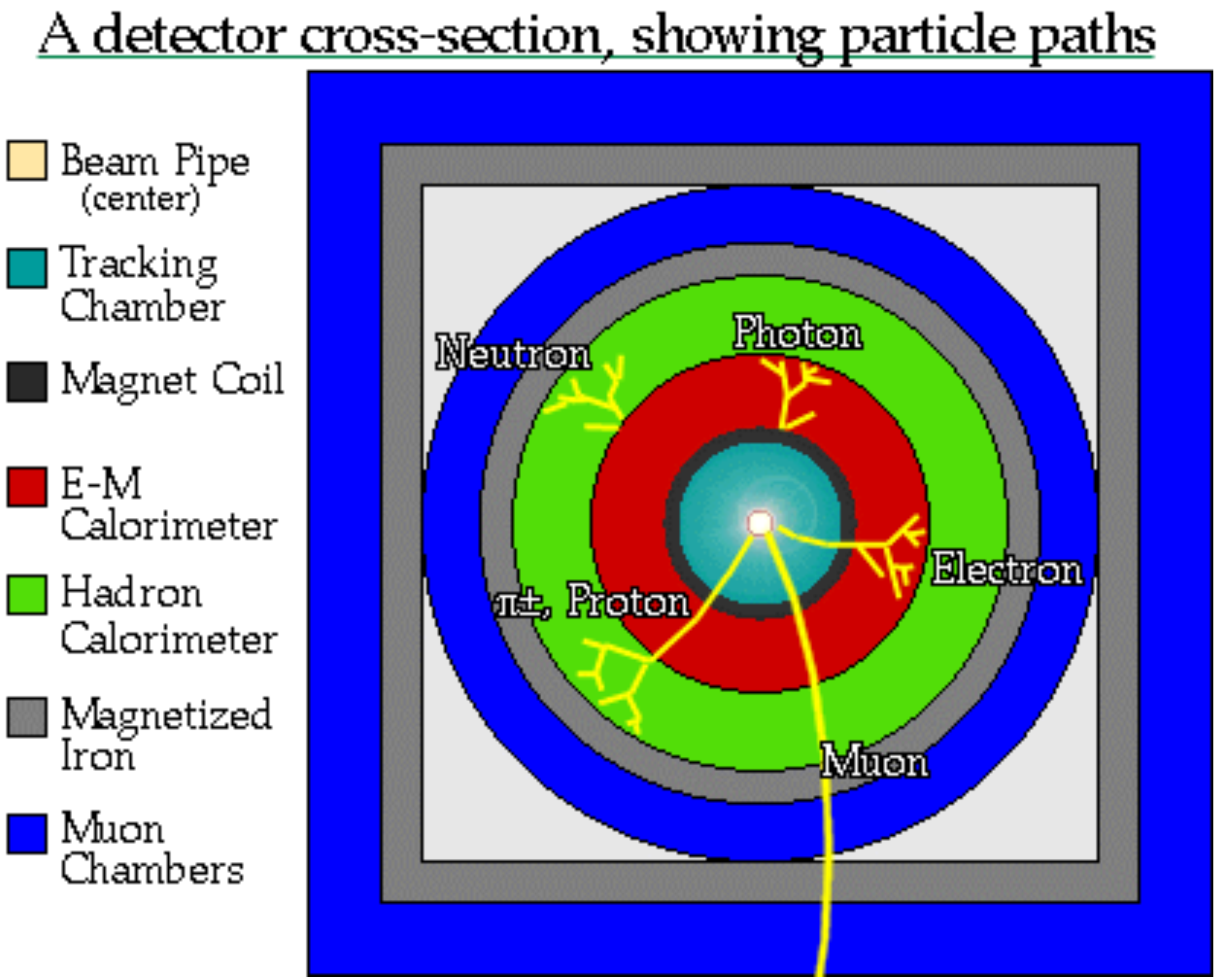

- Layers of Detector Systems around Collision Point

Solid State Detectors

- Specifically
  - microstrip & pixel trackers
- Have become trackers of choice (if affordable)
  - high spatial resolution
  - radiation hard
    - rely on development of micro-electronics fabrication techniques
- Central to heavy flavour tagging, lifetimes
  - vertex detection
    - B flavour
    - Top
    - Higgs

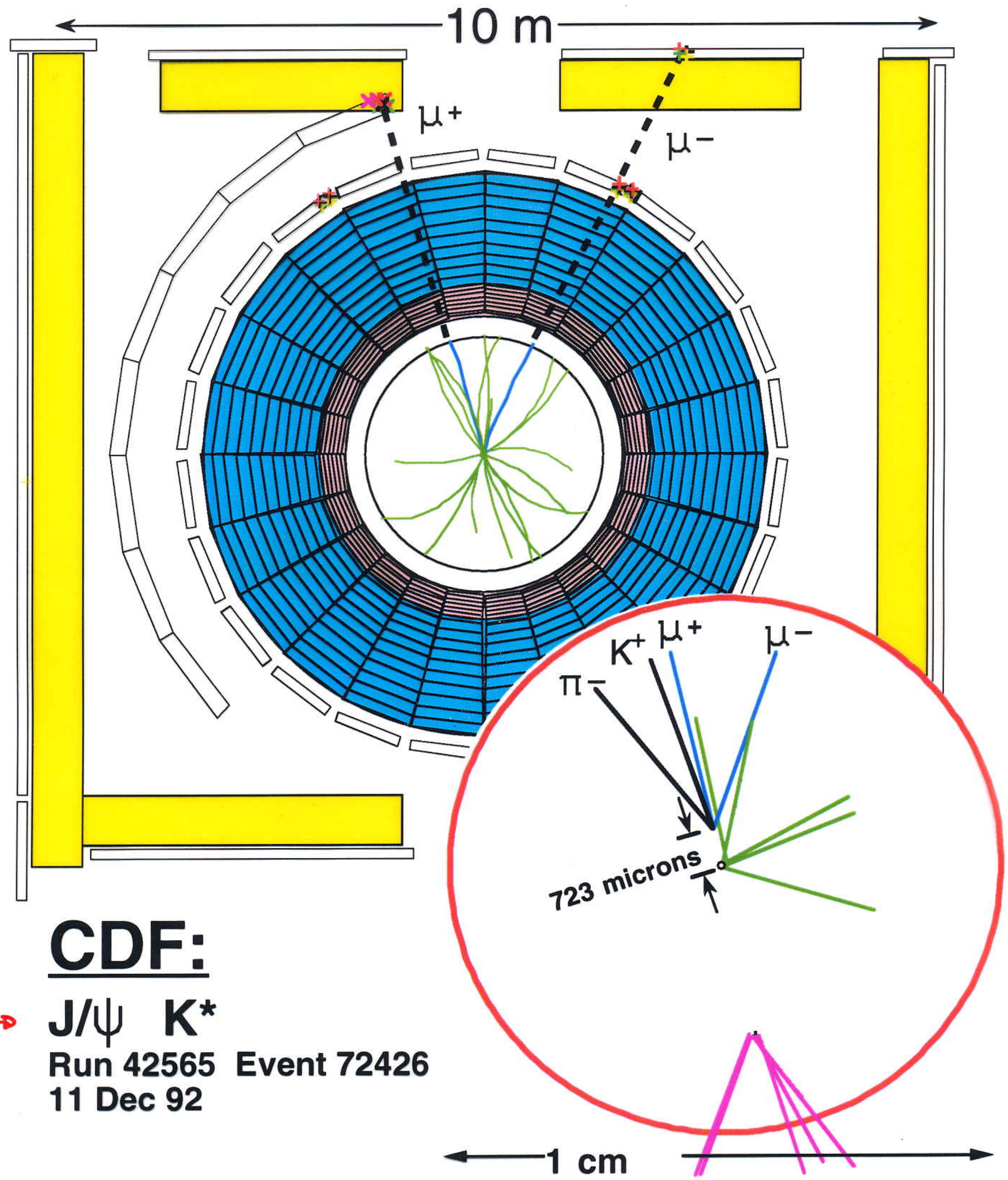

CDF:

B° → J/ψ K*

Run 42565 Event 72426

11 Dec 92

Top Quark Discovery at CDF

e + 4 jet event

40758_44414

24-September, 1992

TWO jets tagged by SVX

fit top mass is 170 +- 10 GeV

e^+, Missing E_t, jet #4 from top

jets 1,2,3 from top (2&3 from W)

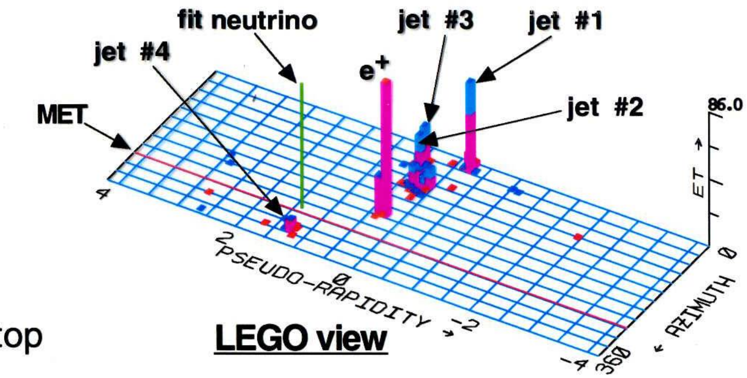

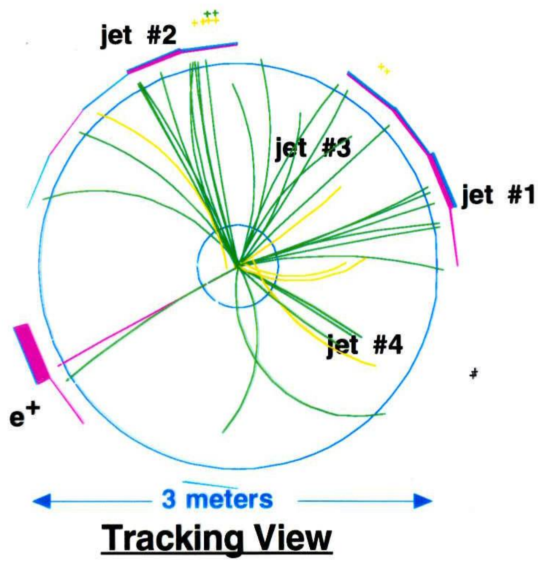

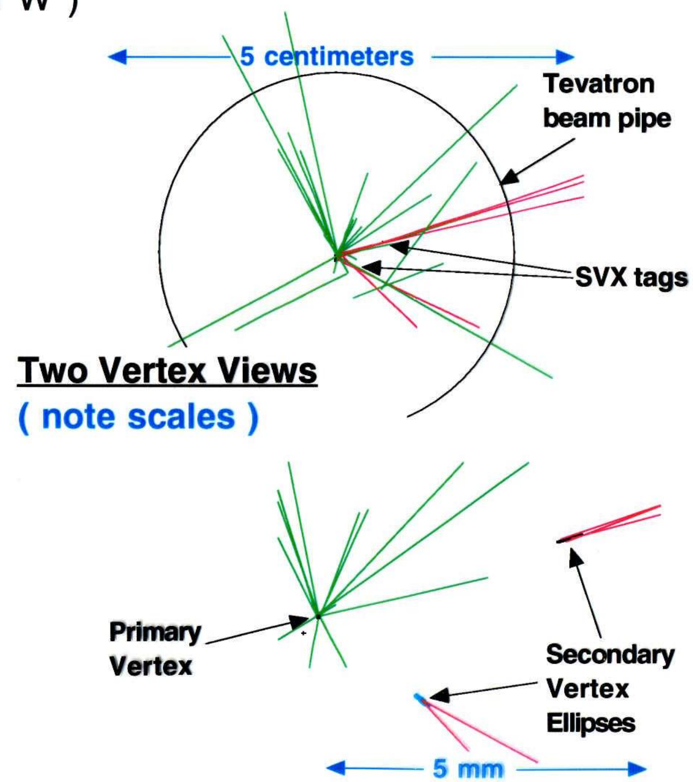

Semiconductors

- Have a large energy gap

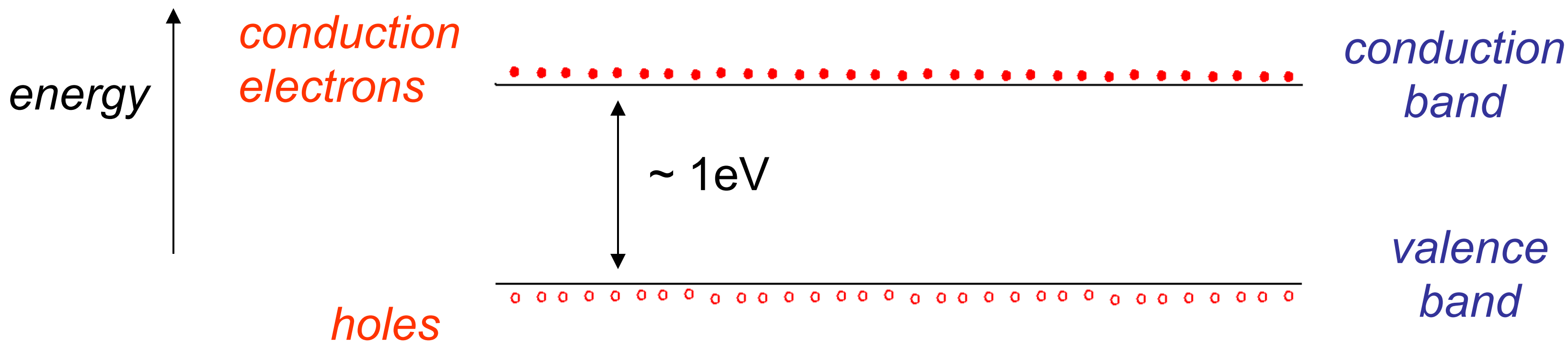

- Small number of charge carriers in conduction band
    - electrons thermally excited across the band gap

$$n_i = AT^{3/2} \exp\left(\frac{-E_g}{2kT}\right)$$

$n_i = 1.5 \times 10^{10}\, cm^{-3}$ in pure silicon at room temp

increases with temperature

Doped Semiconductors

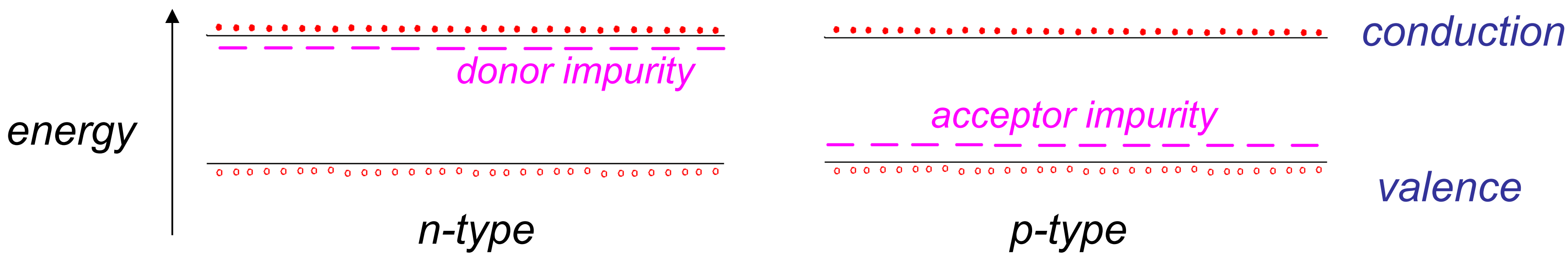

- In n-type , extra conduction electrons easily excited into conduction band

-increase conductivity

- In p-type, valence electrons excited into impurity band – holes in valence band conduct

  - n-type - electrons – majority carriers
  - p-type - holes – majority carriers

p-n Junction

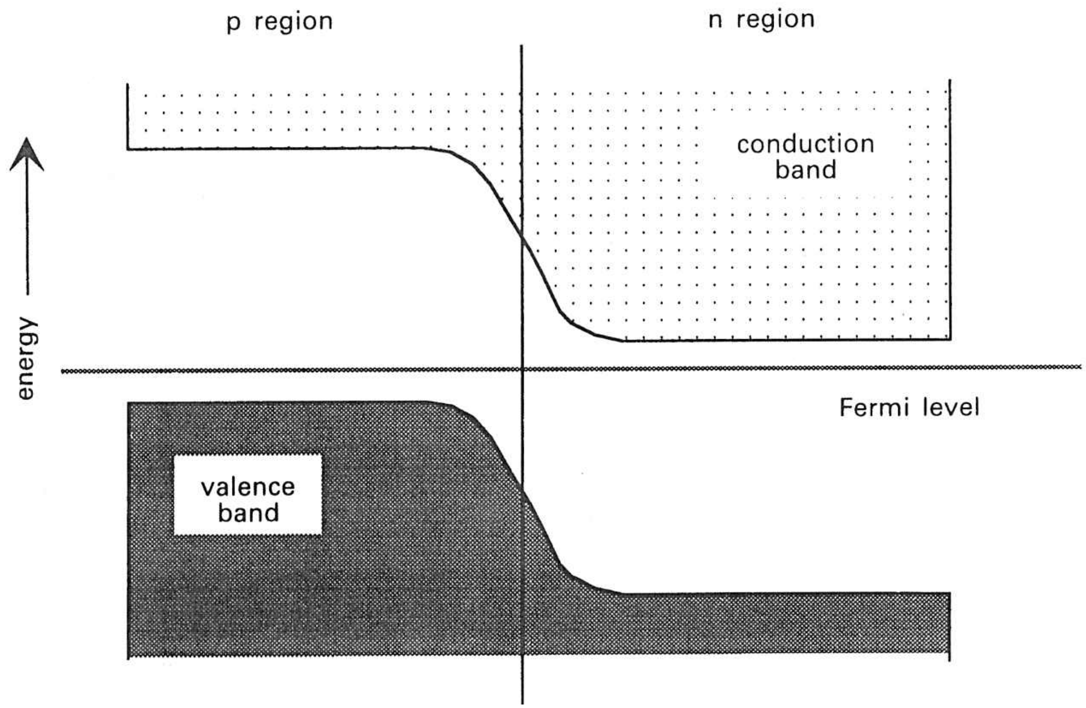

p region
n region
conduction band
energy
Fermi level
valence band

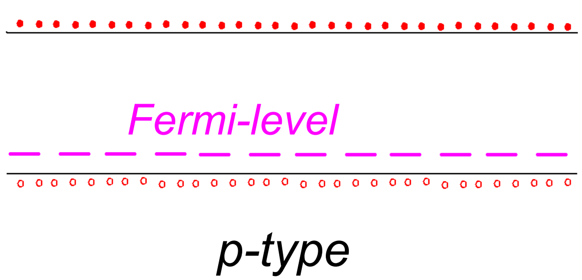

Fermi-level
p-type

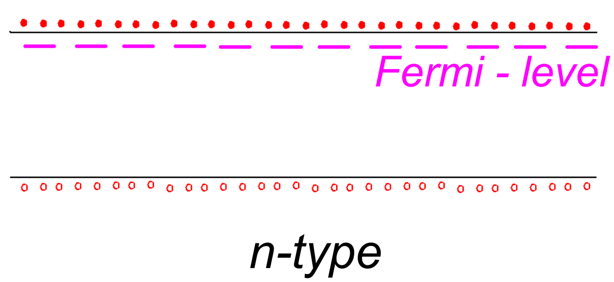

Fermi - level
n-type

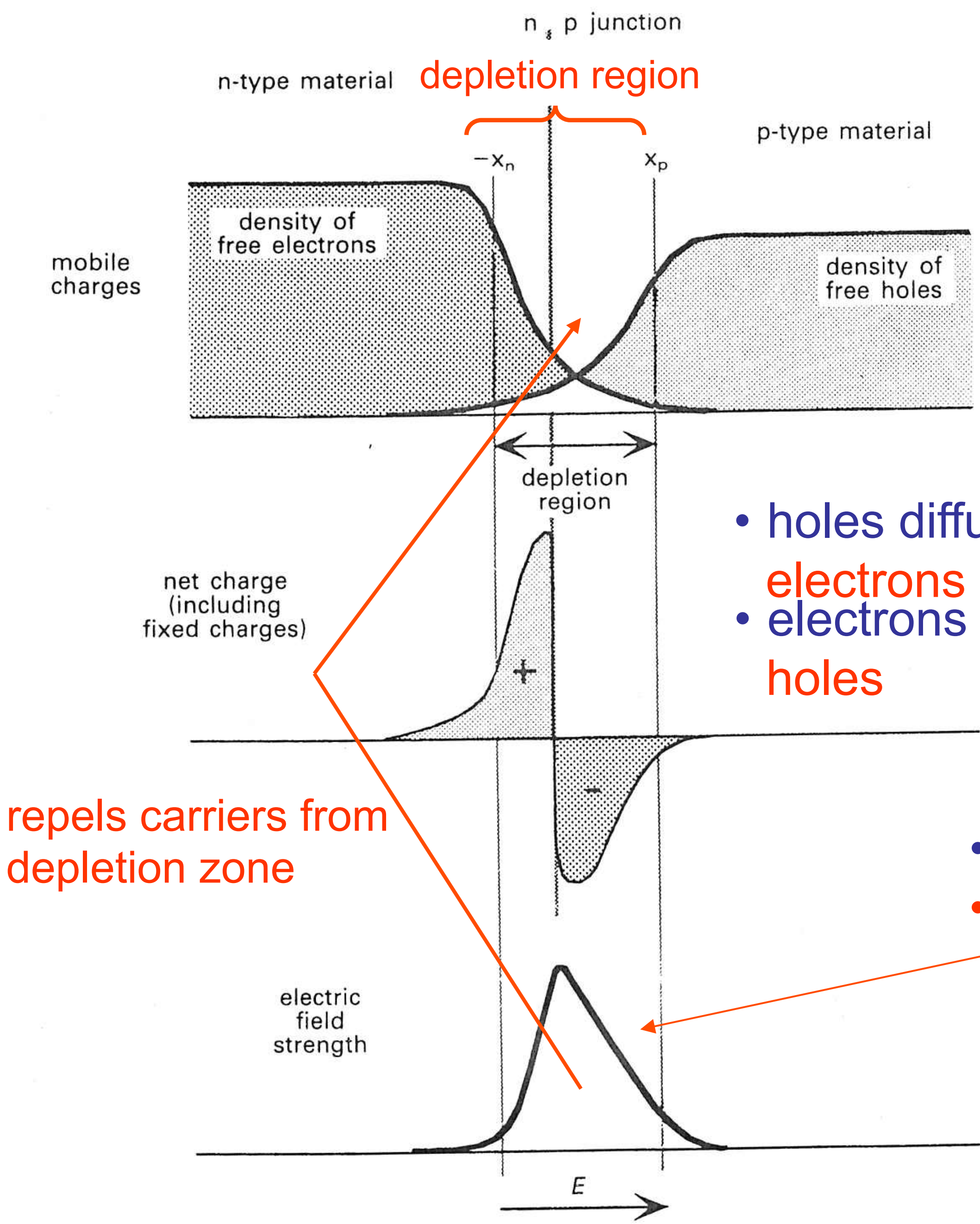

- Both n & p are initially electrically neutral

- holes diffuse into n-region - “fill” electrons
- electrons diffuse into p-region - “fill” holes

⇓

- charge buildup
- electric field

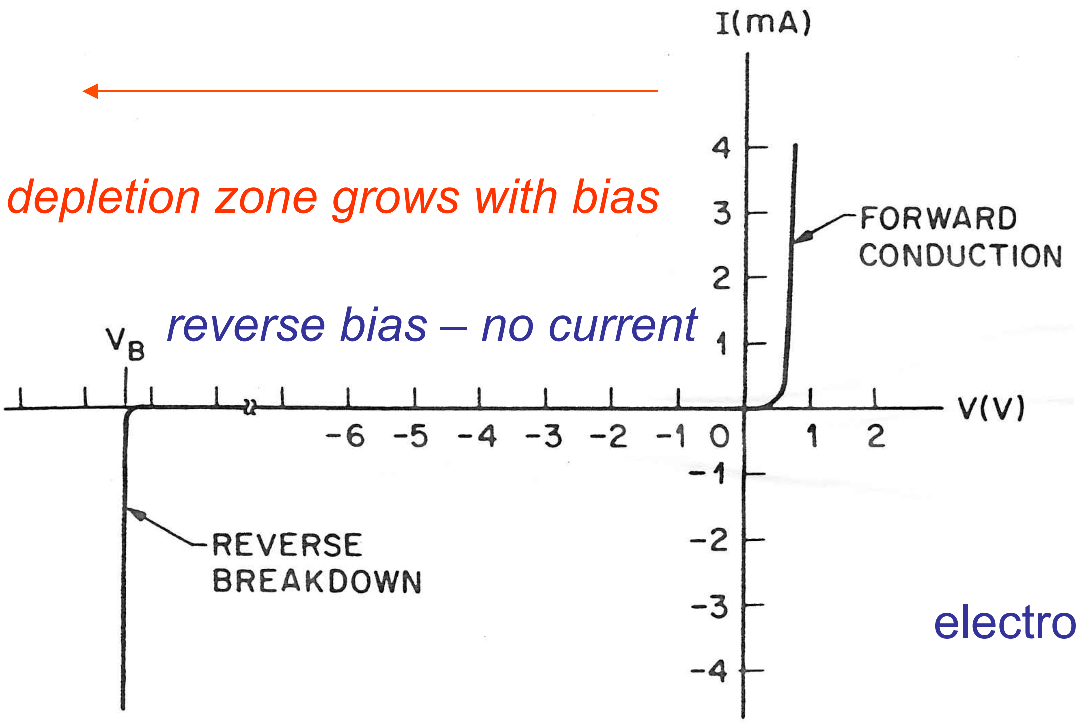

majority carrier current

electrons and holes have different mobility

$$\mu_H = \tfrac{1}{3}\mu_e$$

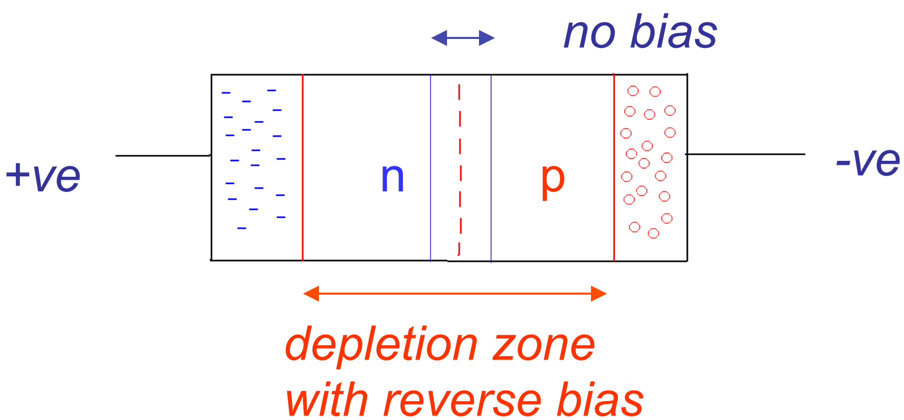

for $V_0 = 300\,V \quad d = 5\,mm$ cf $75\,\mu$

need high resistivity Si for large bias voltage
- high purity or compensated

Depletion Zone as a Detector

- Reverse biased p-n junction – no majority carriers – no current
- Ionizing particle passing through depletion zone
- Liberates electron-hole pairs – current flows
- Intrinsic field not high enough to efficiently collect carriers – small signal
- Small depletion layer – large capacitance – large noise into electronics

- Depth of Depletion Zone

$$d = \left[2\varepsilon \mu_e \rho \left(V_0 + V_B \right) \right]^{\frac{1}{2}}$$

dielectric constant (ε): $1.054\times 10^{-12} \frac{F}{cm}$

electron mobility (μ_e)

resistivity (ρ)

contact (V_0): $V_0 \approx 1V$

bias (V_B)

Principle of micro-strip Detector

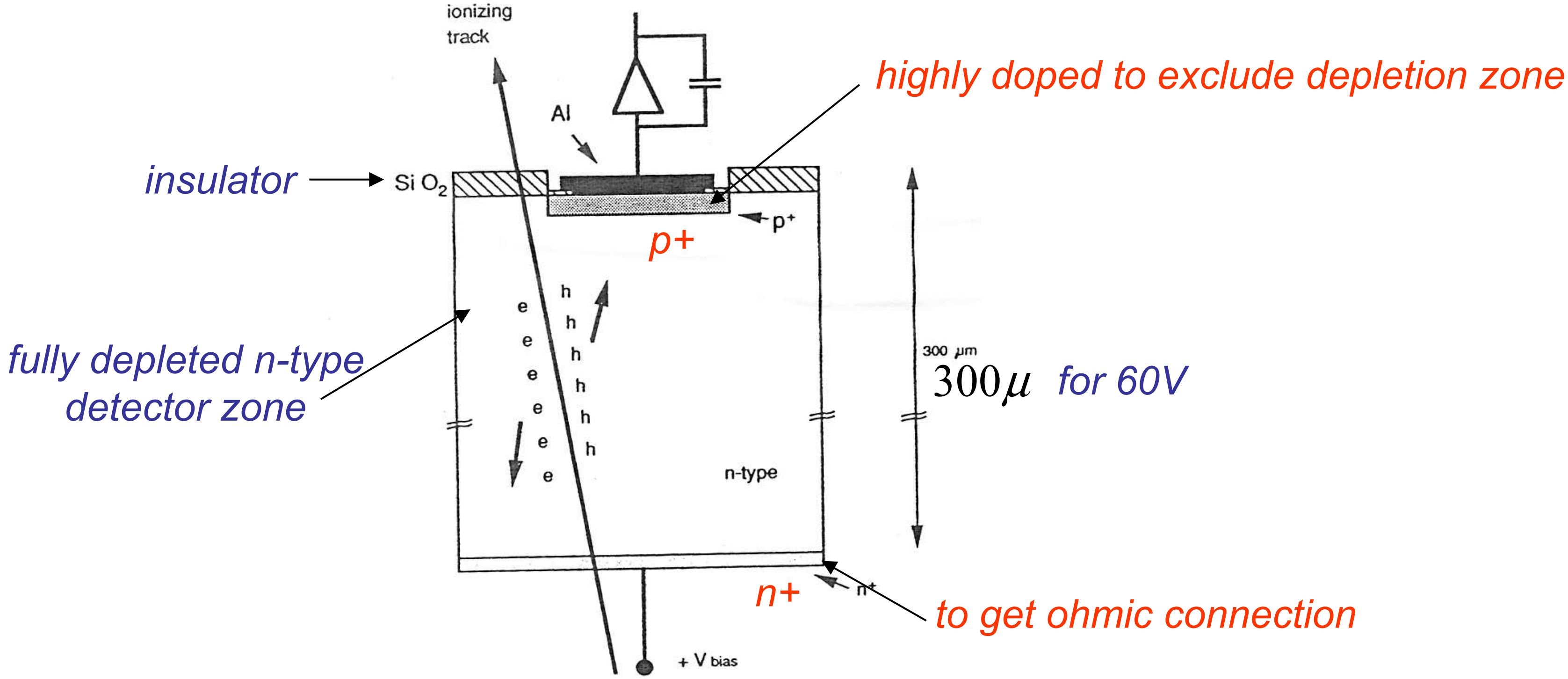

- 1 e-h pair / 3.6 eV - 10^2 e-h per micron - dense
- unlike gas – no multiplication of primary ionization 3×10^4 for 300μ
- noise reduced by full depletion – reduce capacitance

Fabrication

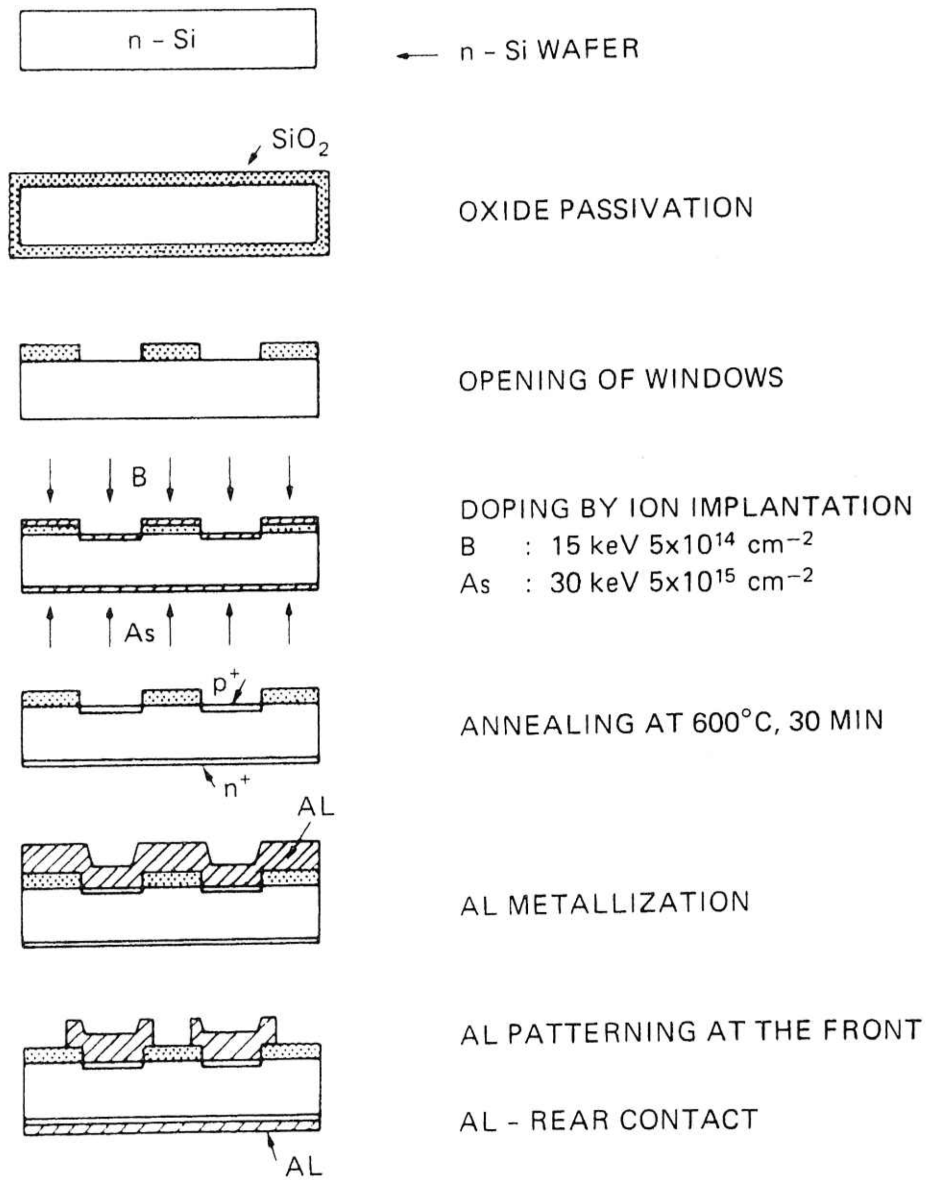

• micro strip structure

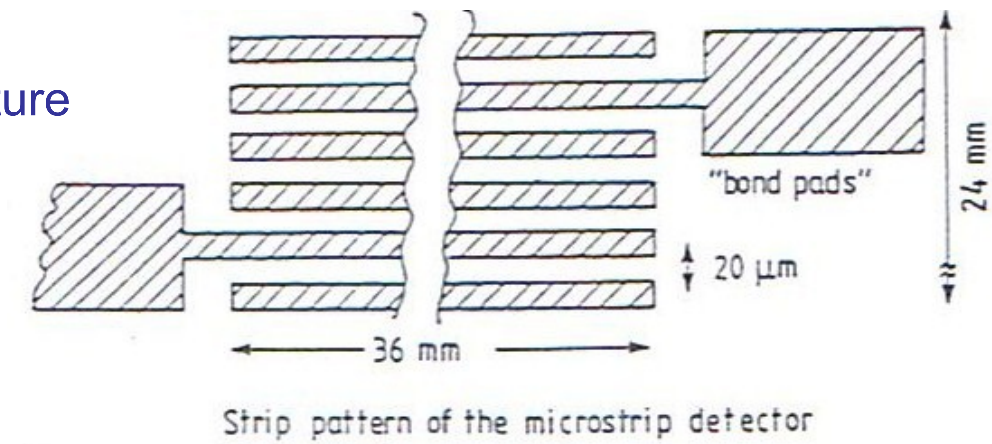

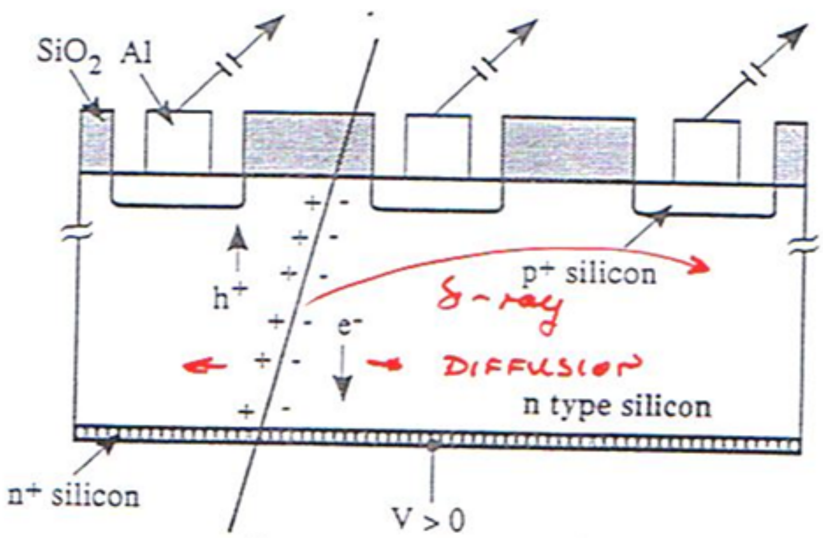

• position resolution < 10 microns

• limited by diffusion and delta-rays

Capacitive Charge - Division

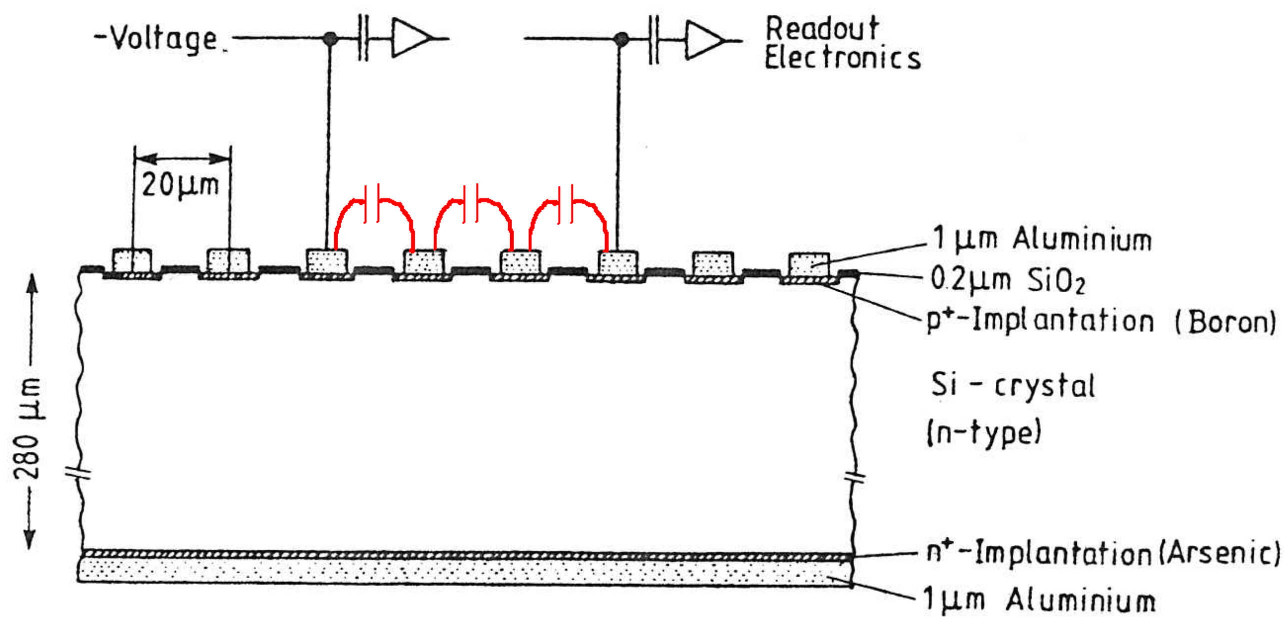

Cross-section of the microstrip detector with capacitative charge division

$$\sigma = \frac{pitch}{\sqrt{12}}$$

- many strips resulting from 20μ pitch
  - ⇨ many electronics channels – many $$
- stray capacitive coupling of strips – read out every n^{th} strip

⇨ read out every 6^{th} strip – effective 120μ pitch -- $\sigma : 8\mu$

Time Development of Signal

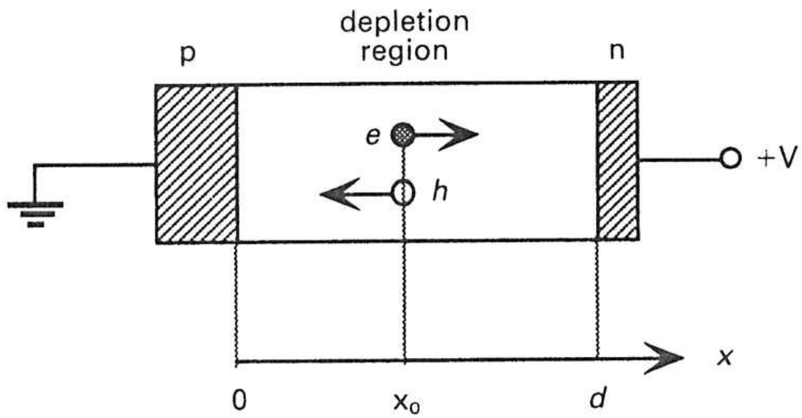

resistivity ρ

dielectric constant ε_s

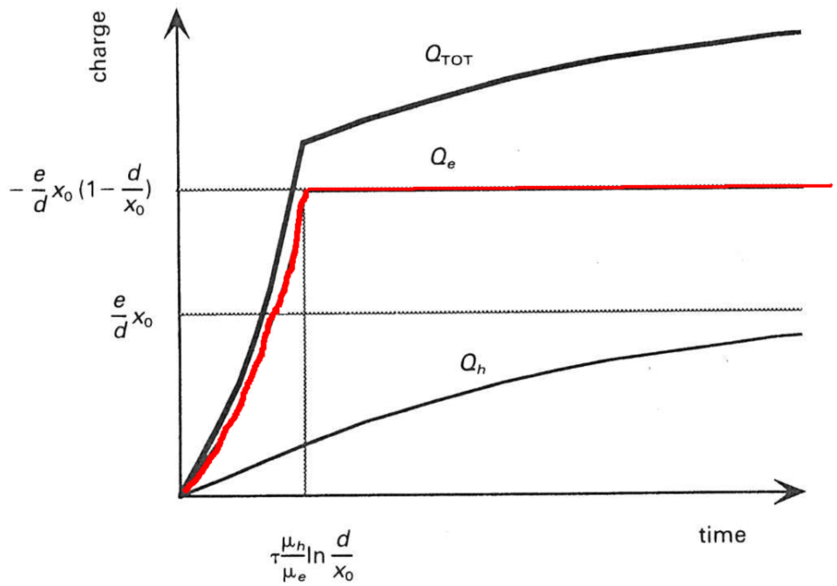

electrons dominate rise time

$$Q_e = \frac{e}{d}x_0\left(1-\exp\frac{\mu_e t}{\mu_h \tau}\right)$$

$$\tau = \varepsilon_s \rho$$

$$Q_h = \frac{e}{d}x_0\left(1-\exp\frac{\mu_h t}{\mu_h \tau}\right)$$

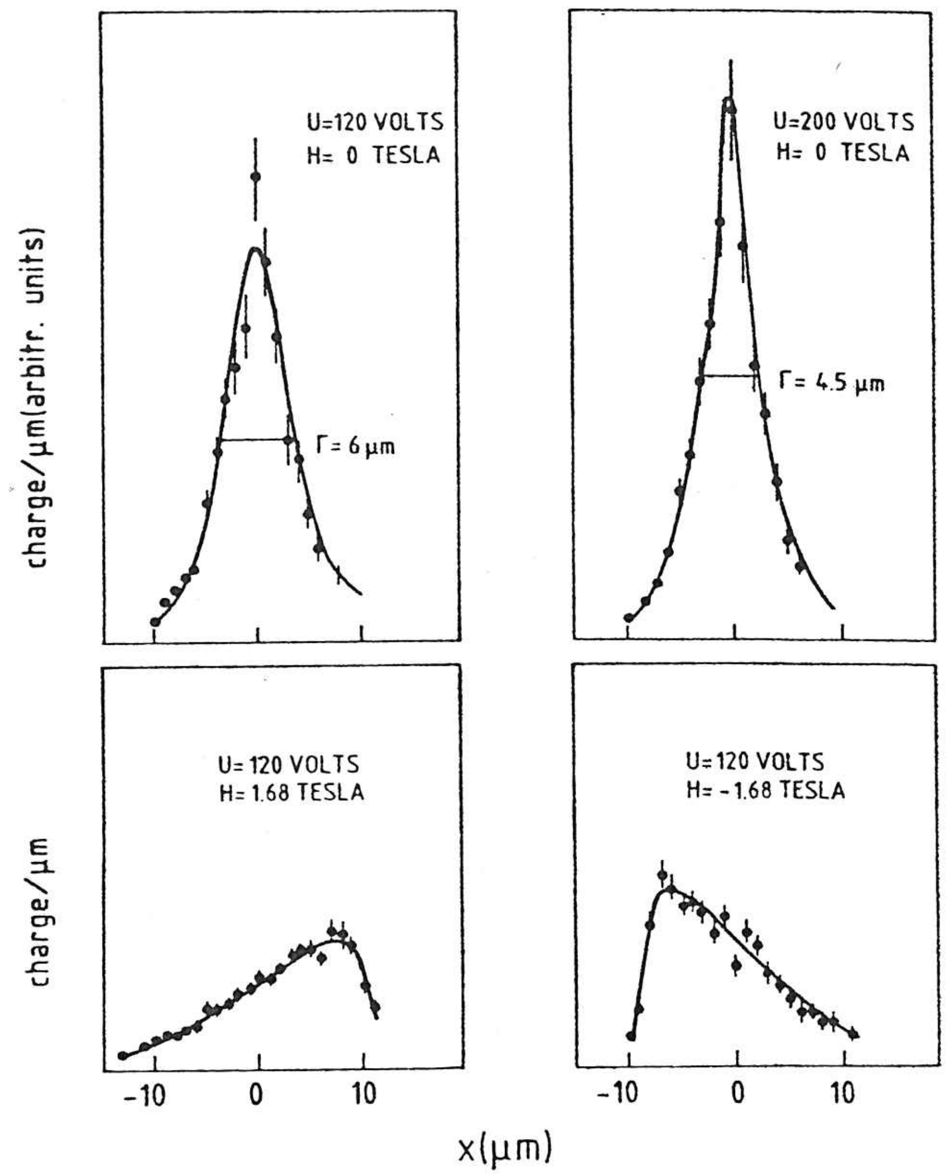

field off

- Effect of magnetic field on space resolution

field on

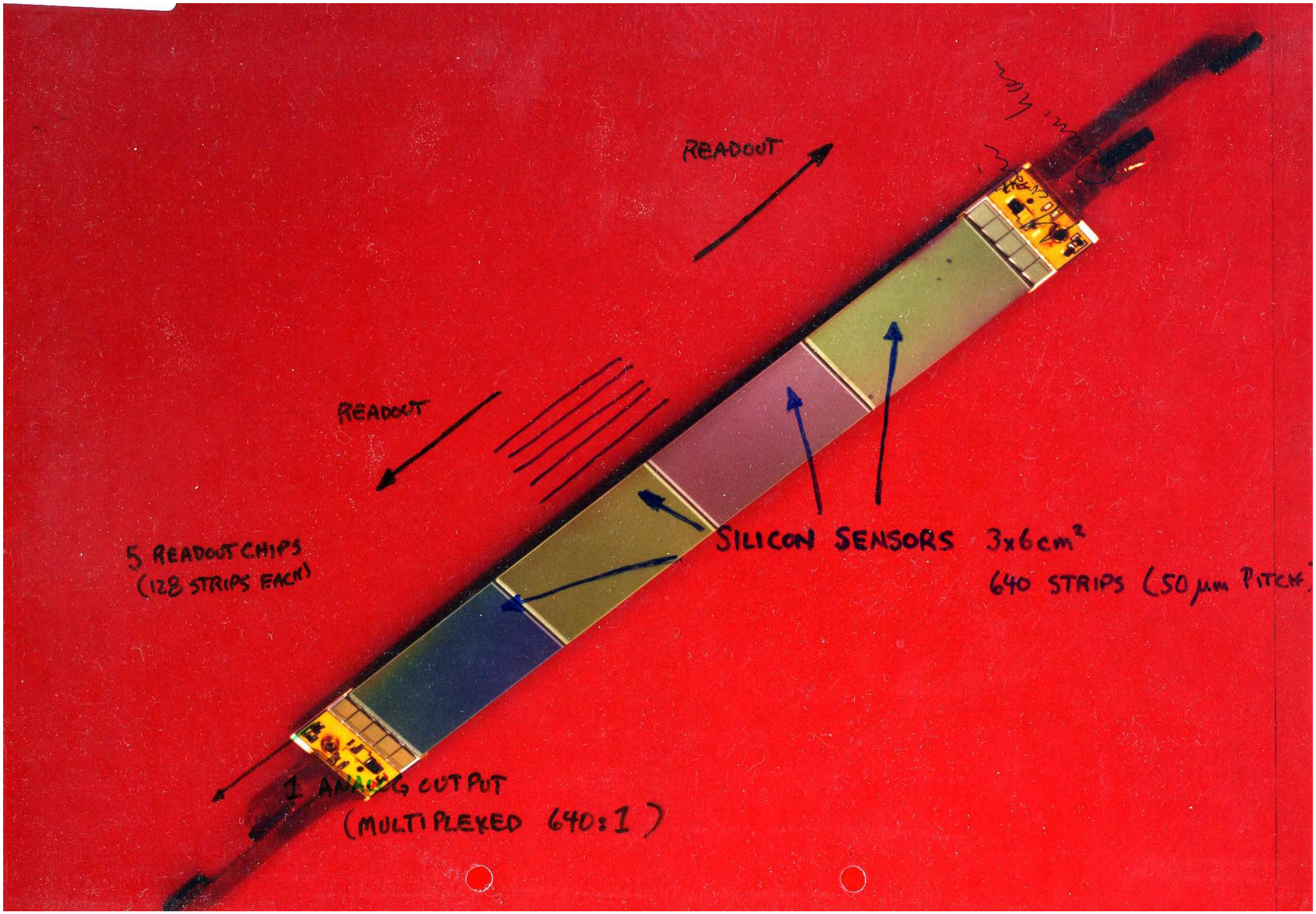
READOUT
READOUT
5 READOUT CHIPS
(128 STRIPS EACH)
SILICON SENSORS 3x6cm²
640 STRIPS (50 μm PITCH)
1 ANALOG OUTPUT
(MULTIPLEXED 640:1)

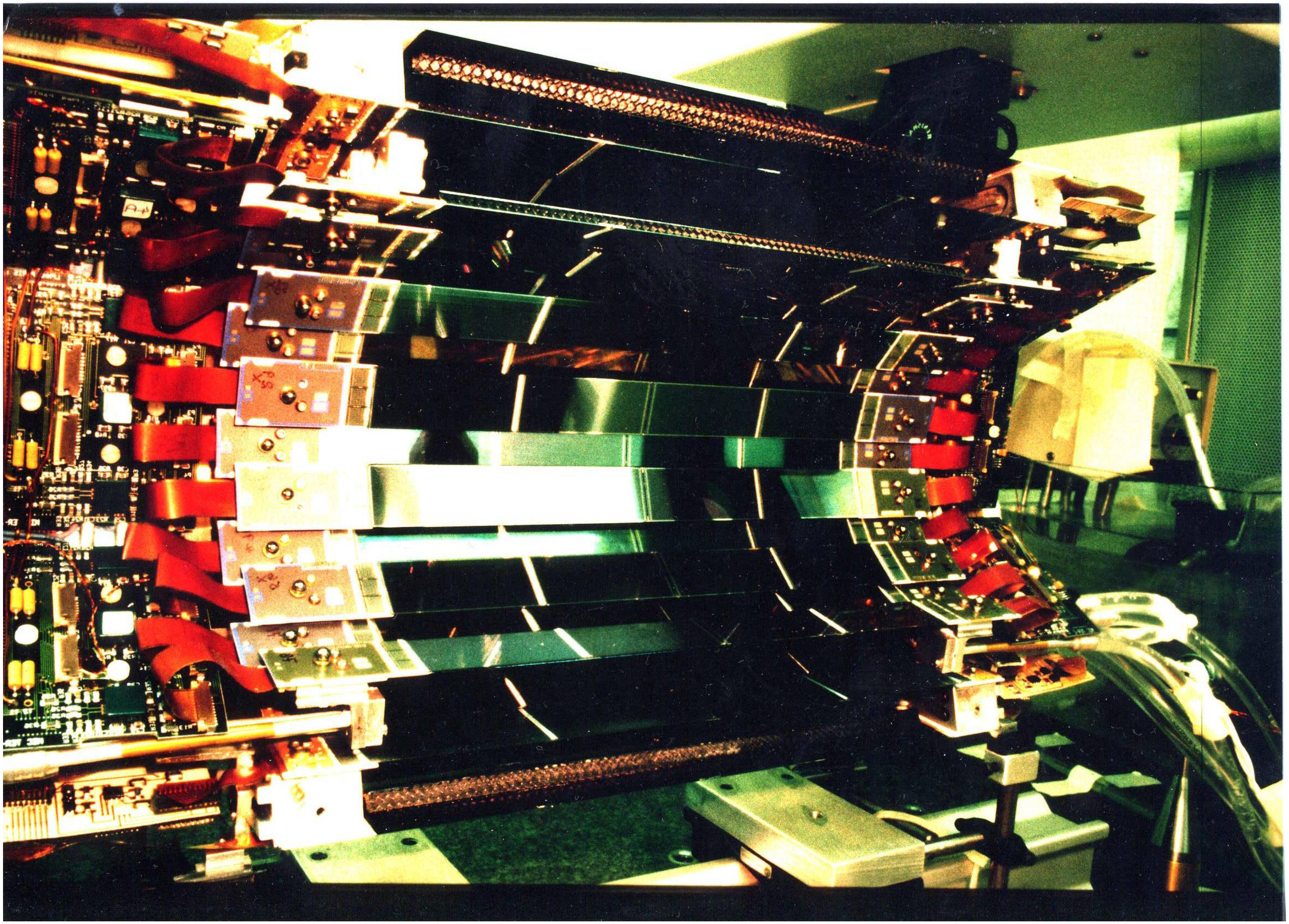

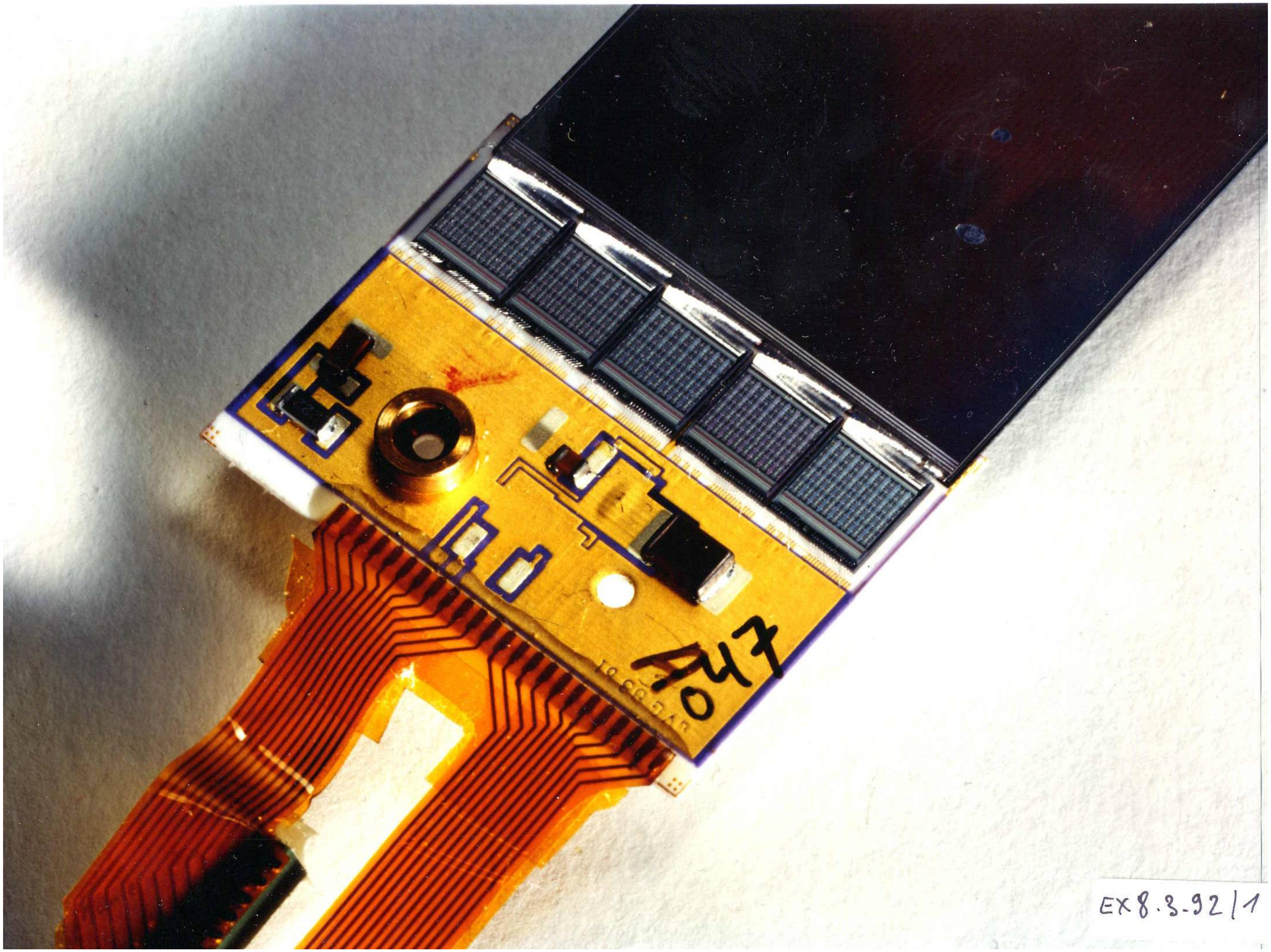
047
EX 8.3-92/1

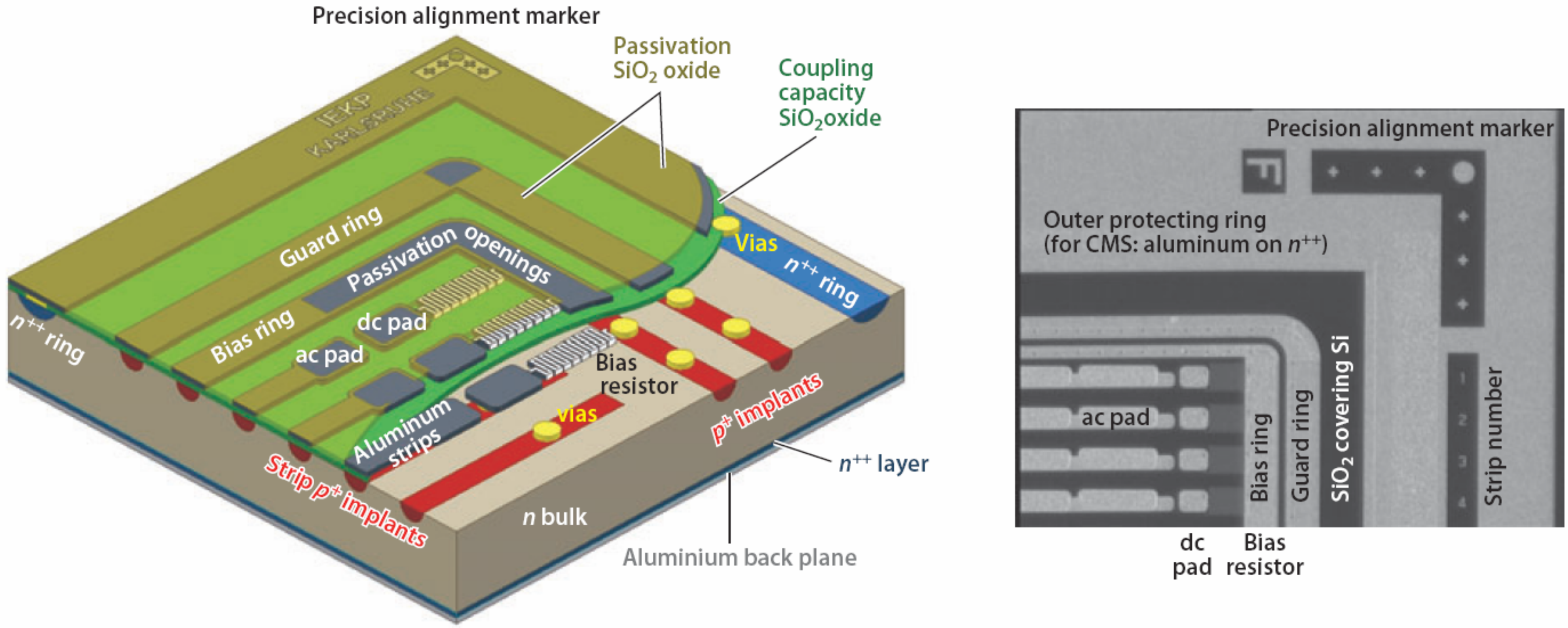

Figure 2

(*a*) Three-dimensional schematic of a single-sided, ac-coupled, polysilicon resistor–biased sensor showing the baseline of the CMS sensor at the LHC. During operation, the bias ring is connected to the GND (ground) potential, which is then distributed via the polysilicon bias resistors to the p^+ implant strips. The aluminum back plane is set to positive high voltage, depleting the full n-bulk volume of free-charge carriers by forming a pn-junction p^+ strip to n bulk. The long strips and thin decoupling oxide allow high coupling capacitances to be implanted directly into the sensor. The guard ring shapes the field at the borders. The n^{++} ring defines the active volume and prevents high field in the edge regions. (*b*) View of an actual sensor surface with a strip pitch of 80 μm.

For personal use only.

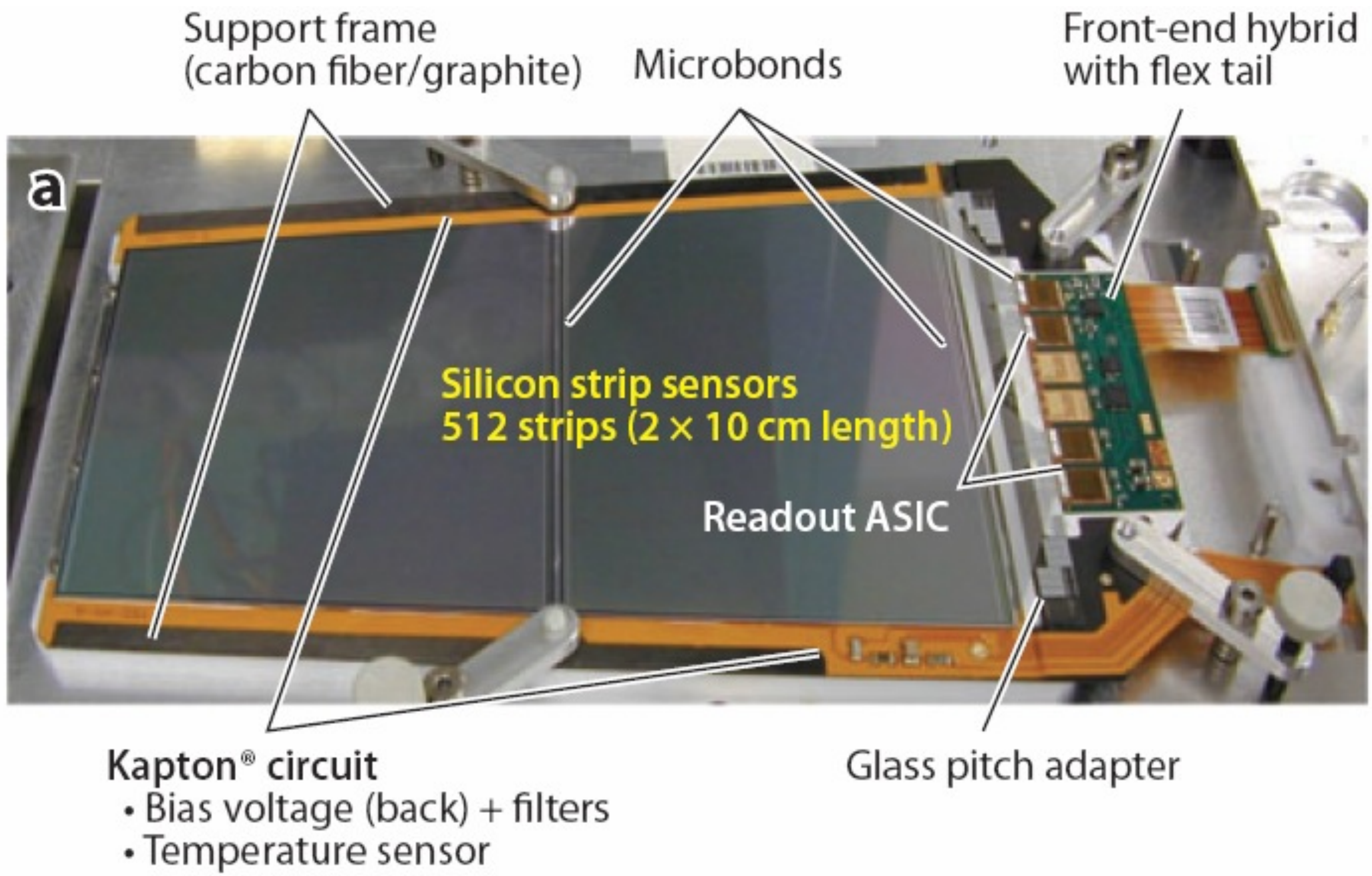

a
Support frame
(carbon fiber/graphite)
Microbonds
Front-end hybrid
with flex tail
Silicon strip sensors
512 strips (2 × 10 cm length)
Readout ASIC
Kapton® circuit
• Bias voltage (back) + filters
• Temperature sensor
Glass pitch adapter

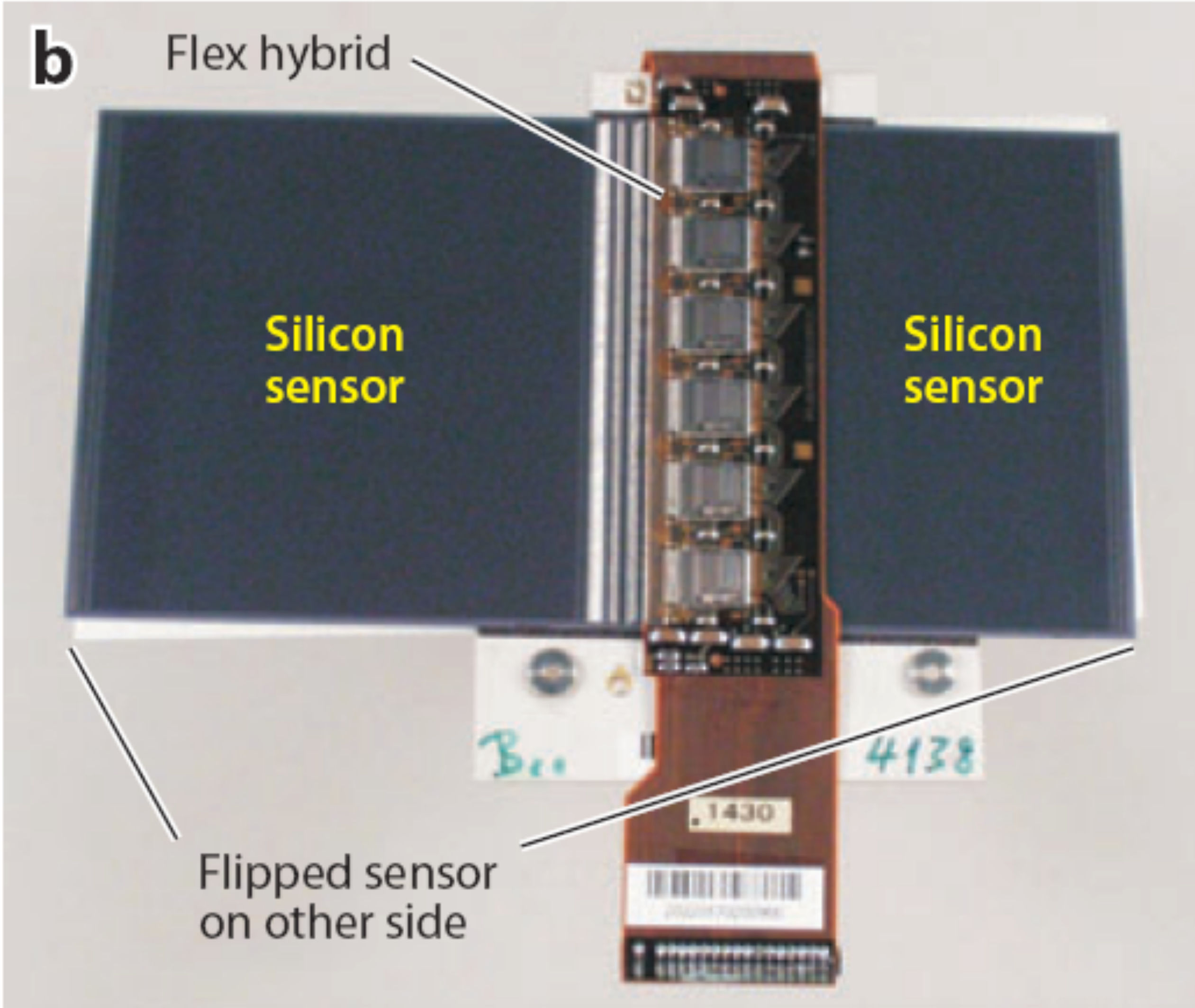
b
Flex hybrid
Silicon sensor
Silicon sensor
4138
1430
Flipped sensor on other side

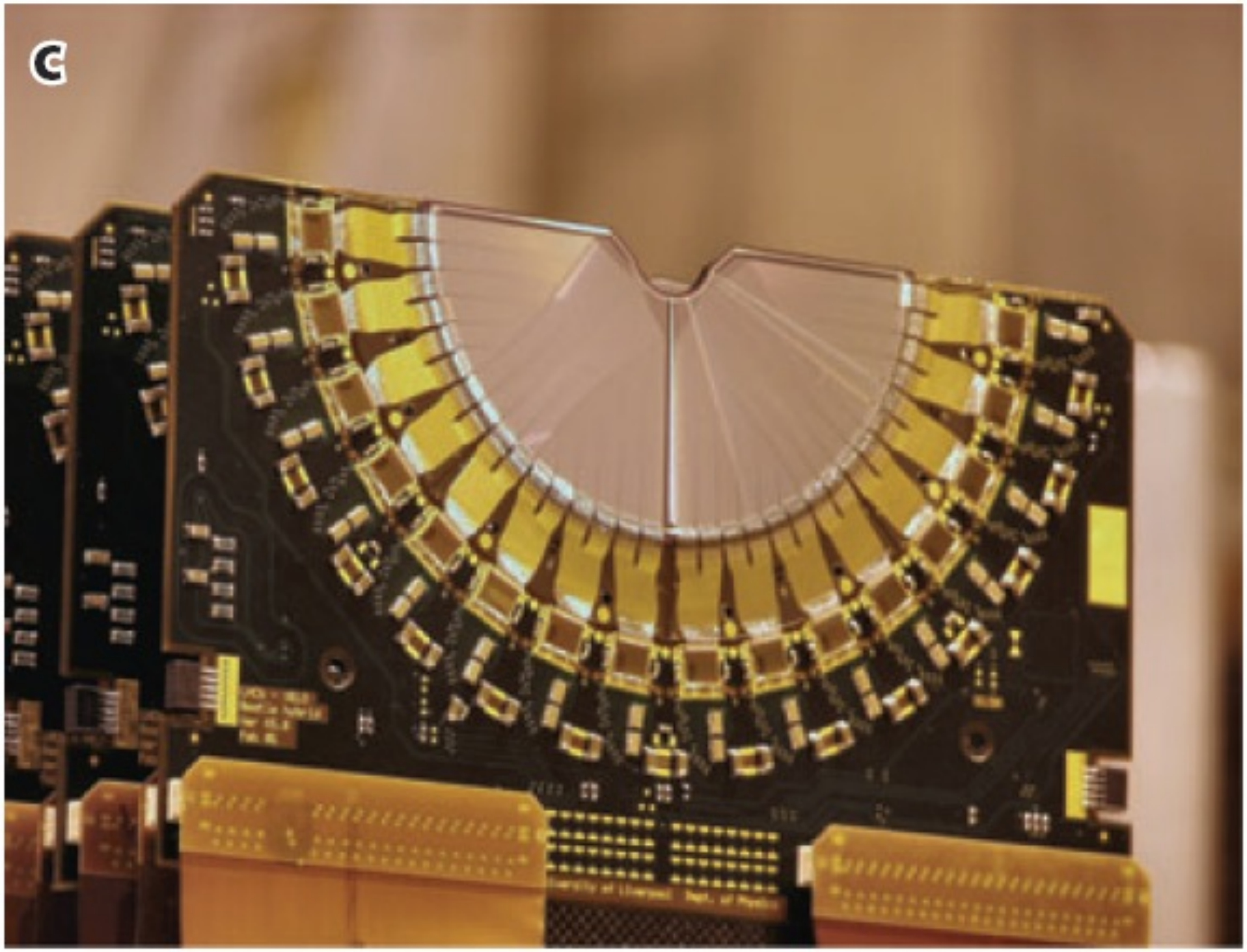
c

The ATLAS Inner Detector

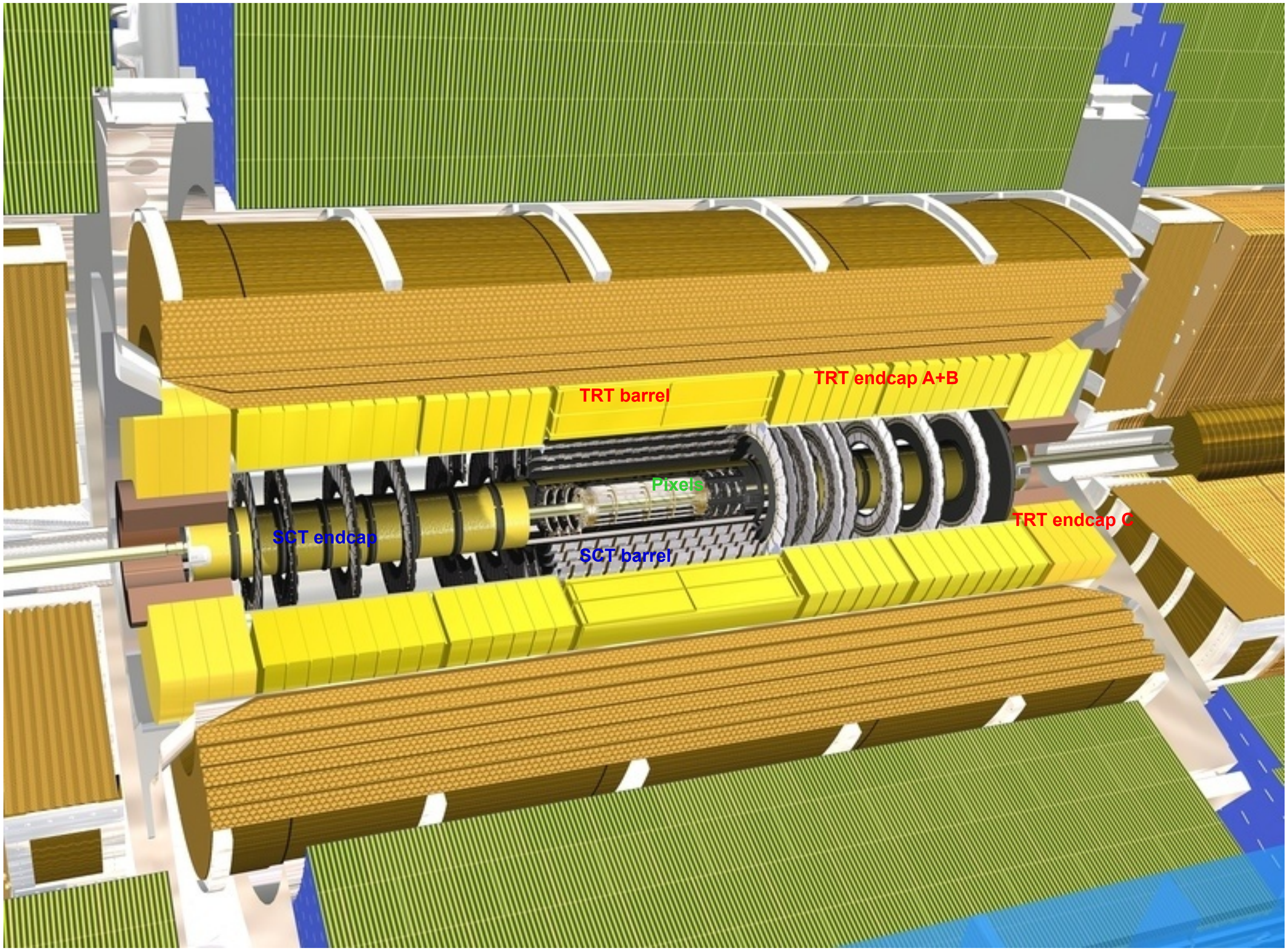

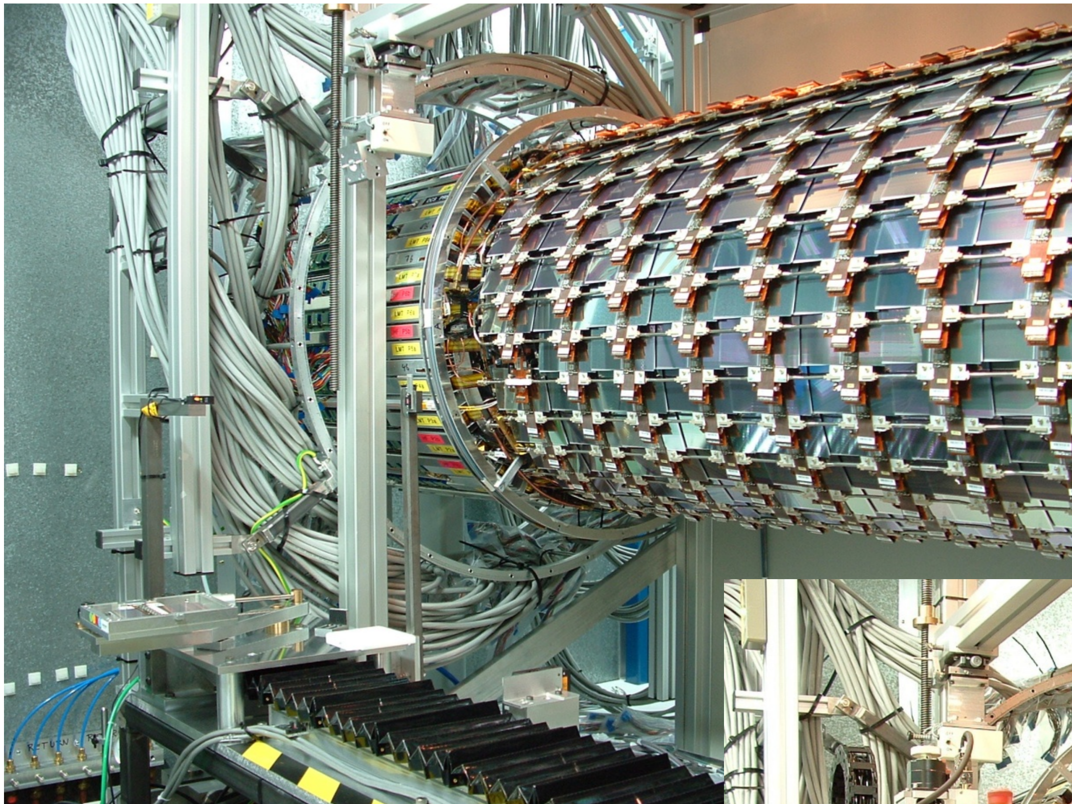

SCT barrel

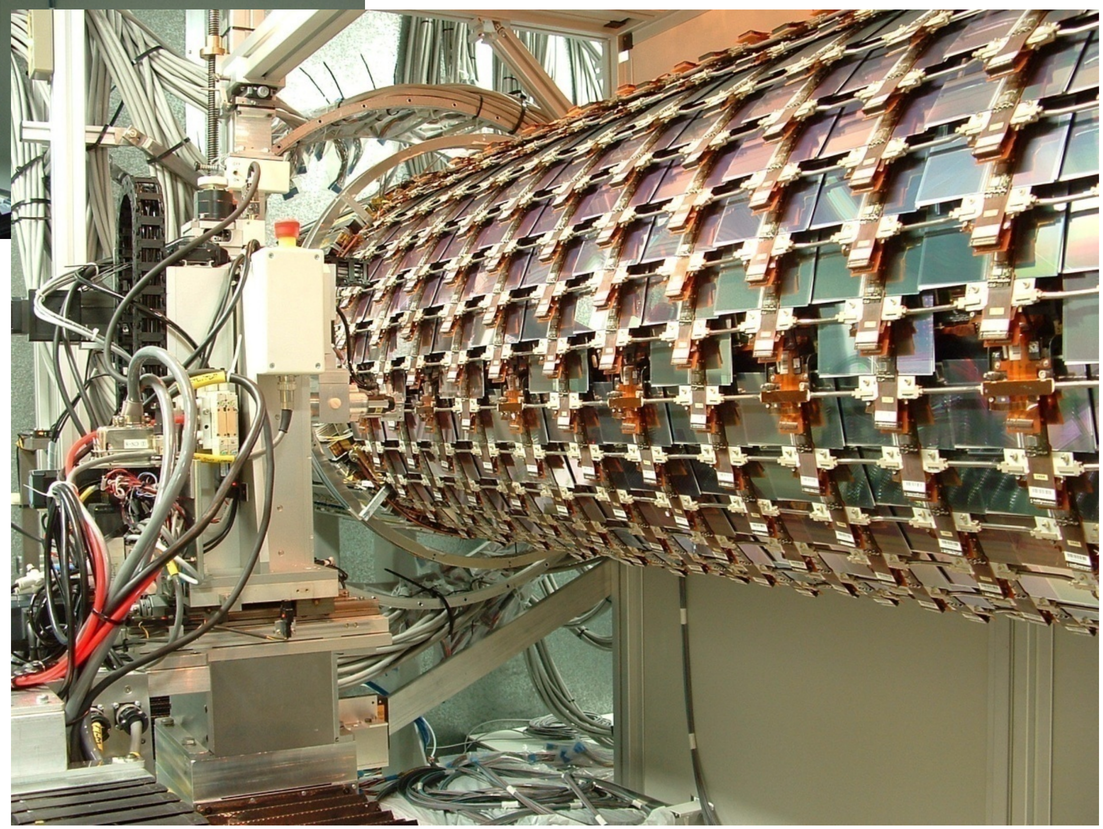

SCT EndCap

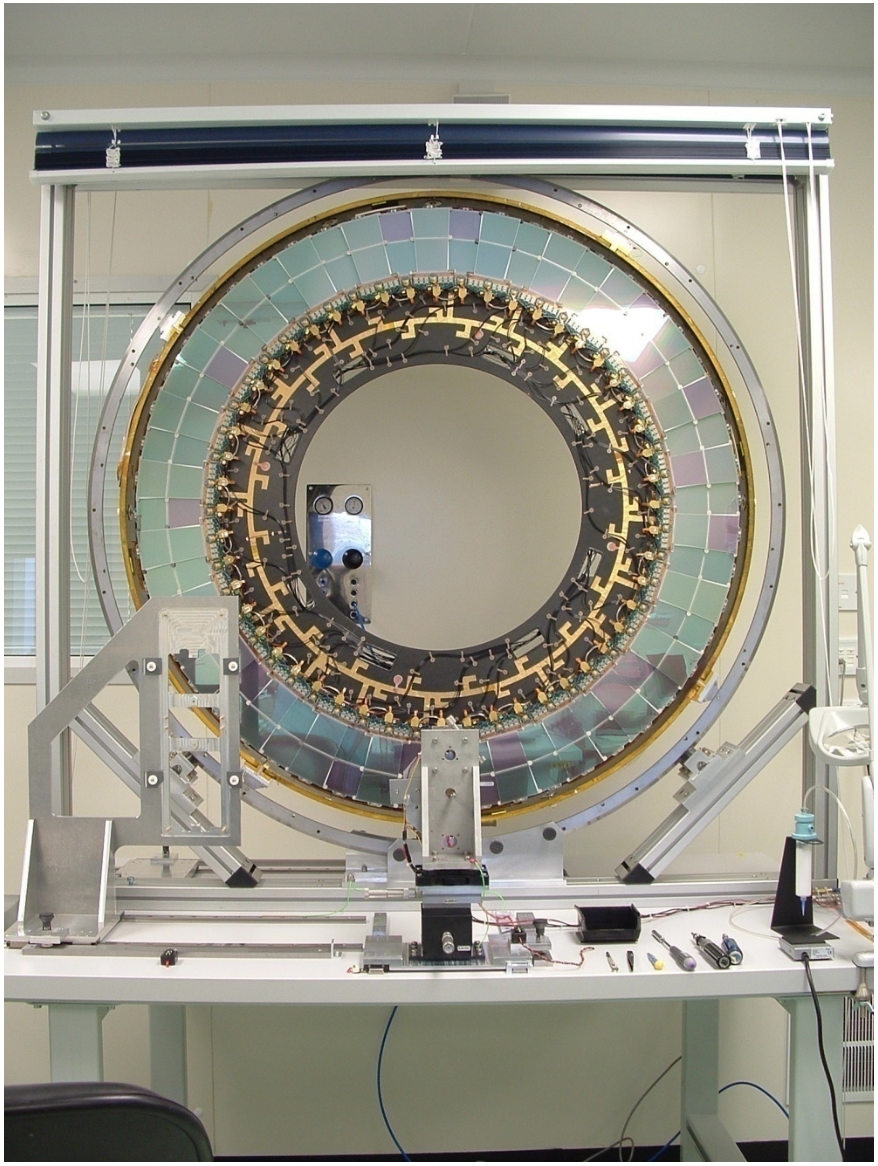

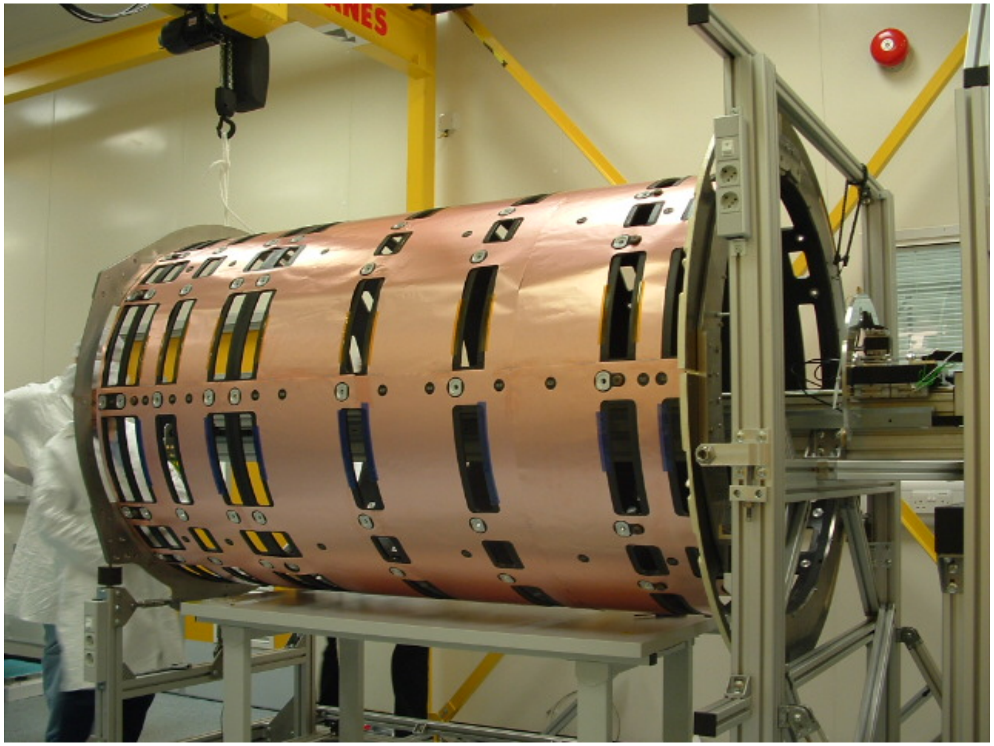

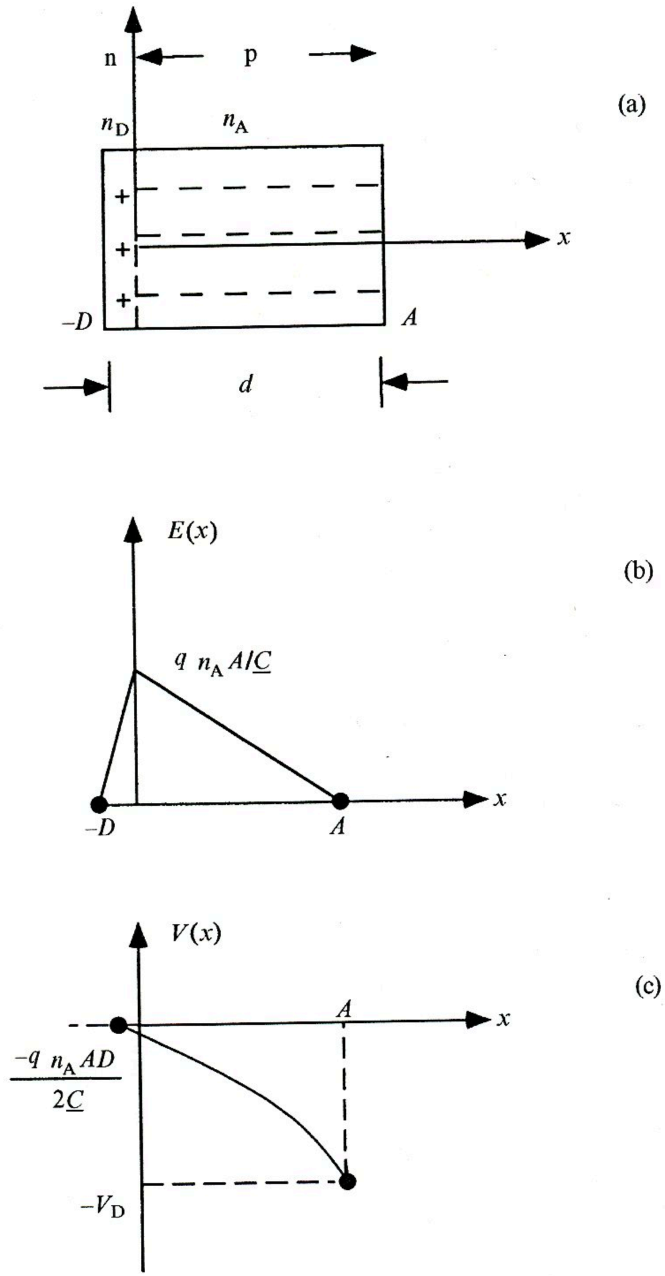

Fig. 9.4. (a) Geometry of a p-n junction. The static charge number density is n_D and n_A. The full depletion region is $d = A + D \sim A$. (b) Electric field for a p–n junction. (c) Electric potential for a p–n junction.

Signal from Si Detector

SAME TREATMENT AS SIGNAL IN GAS TUBE

$$I(t) = \frac{dQ}{dt} = \frac{\mu q_s E^2}{V_B}$$

$$= \frac{4\mu q_s V_B}{d^2} \exp\left(-\frac{2t}{\tau_D}\right)$$

$$= \frac{2 q_s V_B}{\tau_D} \exp\left(-\frac{2t}{\tau_D}\right)$$

$$I(0) = \frac{2q_s}{\tau_D}$$

$$I(\infty) = 0$$

$$\tau_D = \frac{d^2}{2\mu V_D} = \frac{d}{\mu E(0)}$$

- for a source charge q_s ~ *5fC*
- peak electron (hole) currrent *710 nA* (240 nA)
- How does this compare to the noise level?

electron mobility $\mu_e : 1400\, cm^2 V^{-1} s^{-1}$

drift velocity $\sim 42\, \mu ns^{-1}$

for 300μ $\tau_D : 7\, ns$

detector is current source
+
capacitor

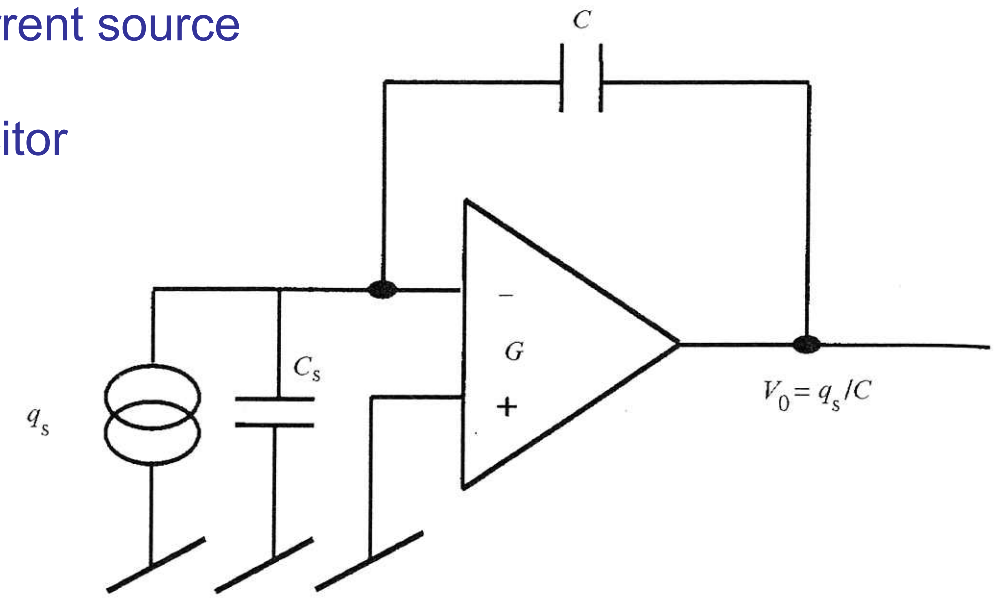

Fig. 9.10. Charge sensitive preamplifier.

$$Q = CV$$

$$I = \frac{dQ}{dt} = C\frac{dV}{dt}$$

$$V_{OUT} \propto q_S$$

NOISE POWER IN A RESISTOR IS THERMAL ENERGY kT SPREAD OVER ALL FREQ. ω

THERMAL NOISE POWER → I_T

$$P = VI = I^2 R \rightarrow dI_T^2 = \frac{2kT}{R}\left(\frac{d\omega}{\pi}\right)$$

($\frac{d\omega}{\pi}$ ↔ df)

SHOT NOISE → QUANTIZED q AT ALL ω

$$dI_s^2 = qI\left(\frac{d\omega}{\pi}\right)$$

$$R_B = kT/qI_E = 1/g_m$$

Equivalent Circuit of Detector + Amplifier

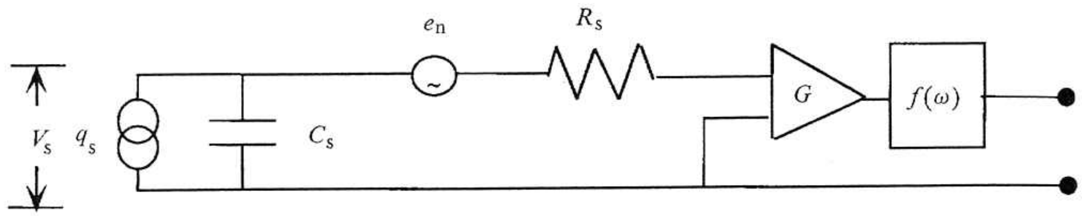

Fig. 9.11. Amplifier and bandwidth limiting filter, $f(\omega)$ with source capacitance, C_s, source resistance, R_s, source charge, q_s, and input noise voltage, e_n.

- resistors – source of thermal noise – thermal energy kT
  - noise is spread uniformly over all frequencies

$$I_T \to P = VI_T = I_T^2 R$$

$$dI_T^2 = \frac{2kT}{R}\left(\frac{d\omega}{\pi}\right)$$ ⇦ *thermal noise*

- current made of – discrete carriers

$$dI_S^2 = qI\left(\frac{d\omega}{\pi}\right)$$ ⇦ *shot noise*

- need to limit bandwidth or infinite noise

9.5 Noise sources – thermal and shot noise 193

- frequency filter

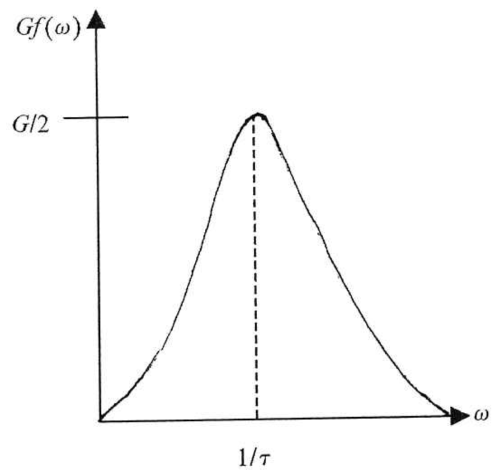

Plot of the transfer function $Gf(\omega)$ which $\rightarrow 0$ as $\omega \rightarrow 0$ and as $\omega \rightarrow \infty$ and $=1/\tau$.

$$f(\omega) = G\left[\frac{\omega\tau}{1+(\omega\tau)^2}\right]$$

$$\sqrt{qI} = 0.4\,nA\sqrt{I\,Hz}$$

$$\sqrt{\frac{2kT}{R}} = 0.9\,nA\sqrt{\frac{Hz}{R}}$$

- for a frequency range of 100 MHz and 1mA
- 126 nA – pretty close to signal

Three sources of noise

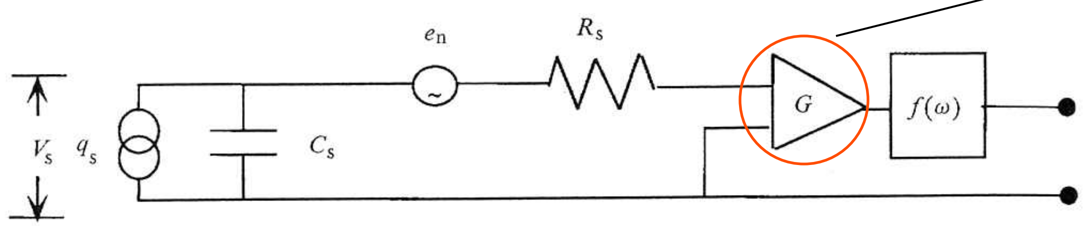

Fig. 9.11. Amplifier and bandwidth limiting filter, $f(\omega)$ with source capacitance, C_s, source resistance, R_s, source charge, q_s, and input noise voltage, e_n.

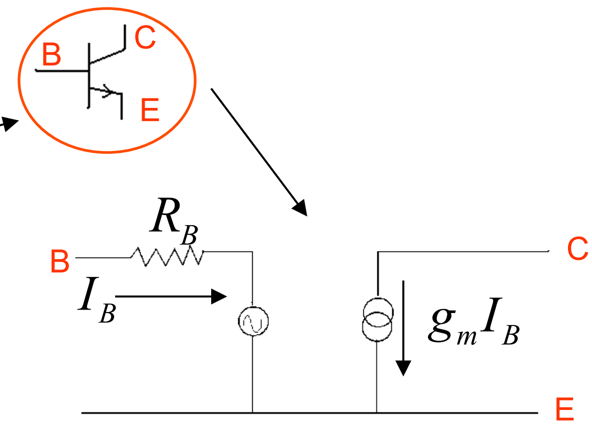

- Thermal – R_S
- Shot - I_E
- Thermal - R_B

$$d\overline{V}^2 = d\overline{I}_T^2 Z_{C_S}^2 + d\overline{I}_S^2 Z_{C_S}^2 + d\overline{I}_T^2 R_B^2$$

$$= \left[\frac{2kT}{R_S (\omega C_S)^2} + \frac{qI_B}{(\omega C_S)^2} + \frac{2kT}{g_m} \right] \left(\frac{d\omega}{\pi} \right)$$

$\frac{1}{\omega^2}$ (first two terms)

constant (third term)

After shaping (filter) Equivalent Noise Charge

$$ENCP = 2.72 \sqrt{\tau \left(\frac{kT}{2R_S} + q\frac{I_B}{4} \right)}$$

$$ENCS = 2.72 C_S \sqrt{\frac{kT}{2 g_m \tau}}$$

- Low temp
- R_S large
- I_B small

} parallel noise

- C_S small
- R_B small

} series noise

$$d\bar{v}^2 = d\bar{I}_T^2 Z_{C_s}^2 + d\bar{I}_s^2 Z_{C_s}^2 + d\bar{I}_T^2 R_B^2$$

$$d\bar{v}^2 = \left[\frac{2kT}{R_s(\omega C_s)^2} + \frac{qI_B}{(\omega C_s)^2} + \frac{2kT}{g_m}\right]\frac{d\omega}{\pi}$$

RMS VOLTAGE

$$\langle v^2\rangle = \int_0^\infty |f(\omega)|^2 \frac{d\bar{v}^2}{d\omega} d\omega$$

$$= G^2\left[\left(\frac{kT}{2R_s} + \frac{qI_B}{4}\right)\frac{\tau}{C_s^2} + \frac{kT}{2g_m\tau}\right]$$

FOR A SIGNAL CHARGE q_s, IF THE FILTER MATCHES THE FREQUENCY DISTRIBUTION OF THE SOURCE

2.72....

$$q_s \rightarrow \frac{q_s G}{C_s} / e = V$$

CHARGE ENC $\rightarrow \left(ENC \cdot \frac{G}{C_s e} \right)^2 \equiv \langle V^2 \rangle$

NOISE CHARGE FROM ALL SOURCES

$$ENC_P = (C_s e/G)\sqrt{\langle V^2 \rangle_P} \equiv e\sqrt{\tau\left(\frac{kT}{2R_s} + \frac{q I_B}{4}\right)}$$

$$ENC_S = (C_s e/G)\sqrt{\langle V_2 \rangle_S} \equiv e\, C_s \sqrt{\frac{kT}{2g_m}\frac{1}{\tau}}$$

P ⇒ $\|^{el}$ RESISTOR ; S ⇒ SERIES RESISTOR

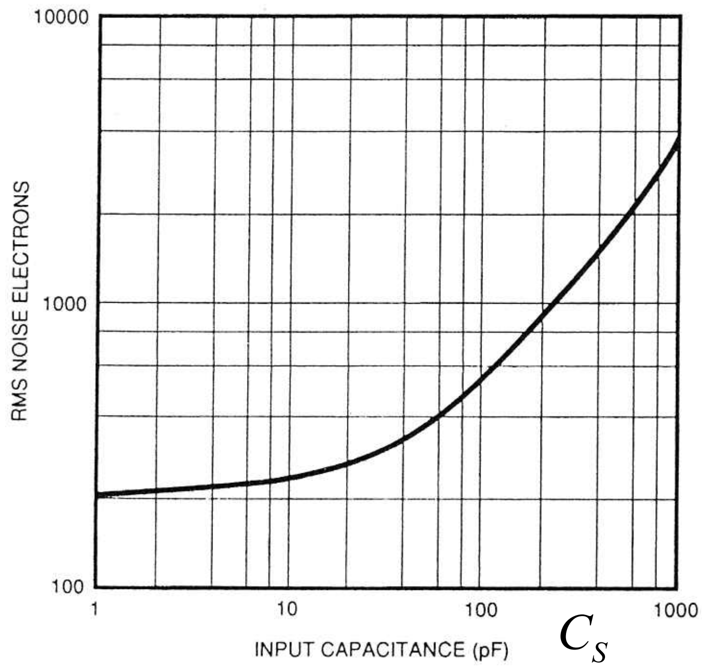

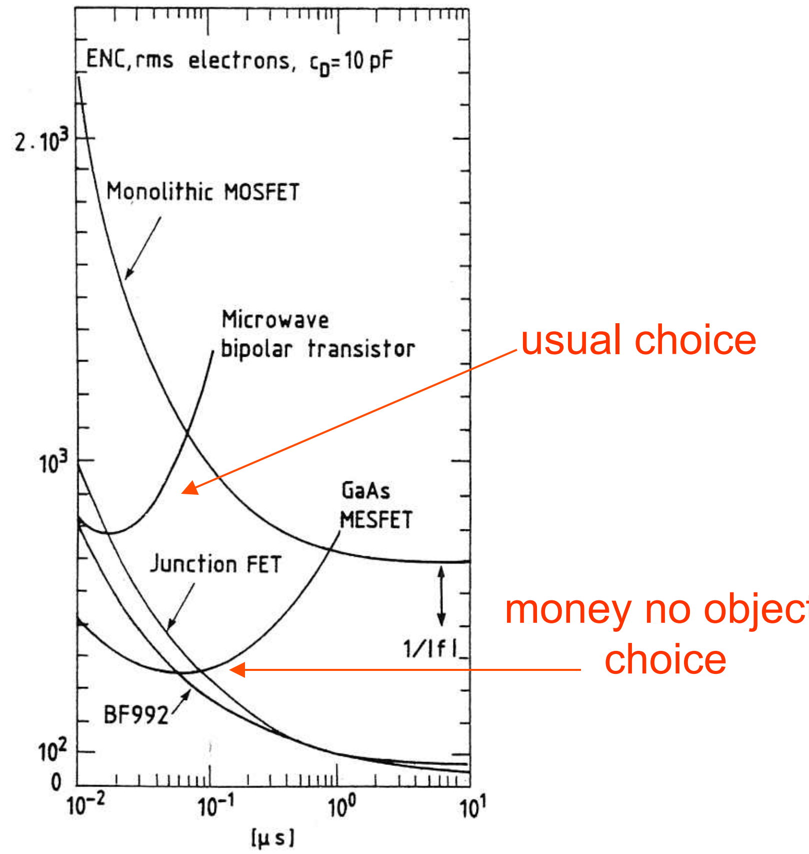

- minimize detector cap – minimize noise
- long strips? – cheap – too noisy

- transistor noise

$$C_S = 25\ pF$$
$$\tau = 25\ ns$$

~ 1000 electrons

cf signal ~ 31000 electrons

Total Noise

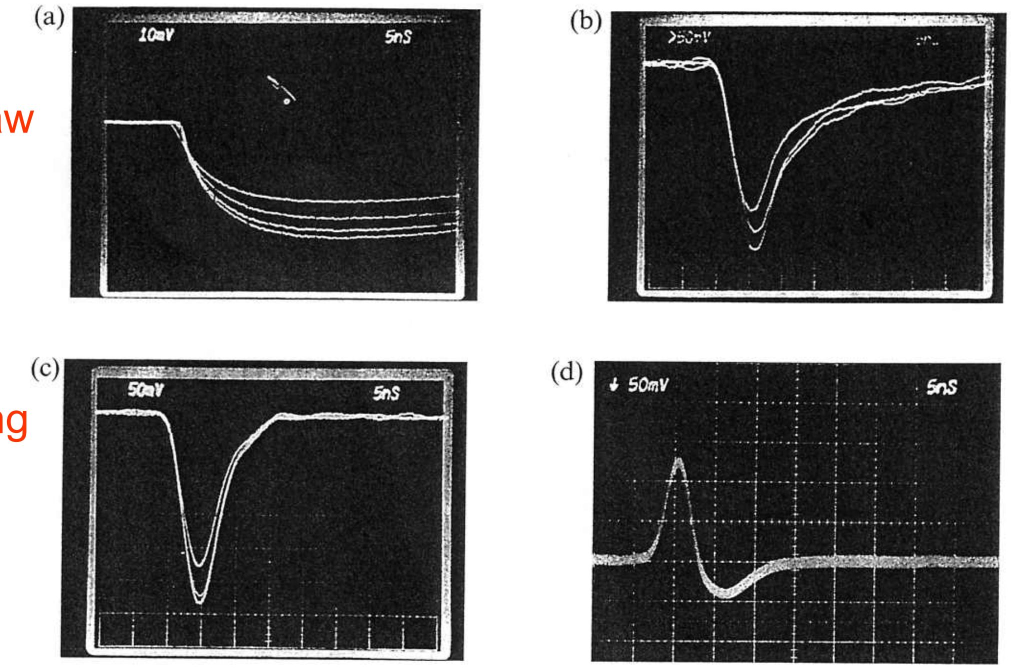

raw

cancel tail

pole-zero shaping

impulse response
- noise

series noise

$q_s : 51\,fC$

$g_m : 25\Omega^{-1}$

$C_S : 30\,pF$

$\tau : 10\,ns$

1125 electrons

parallel noise

$R_S : 1M\Omega$

$I_B : 1mA$

825 electrons

add in quadrature

$$\frac{\text{Signal}}{\text{Noise}} : 23$$

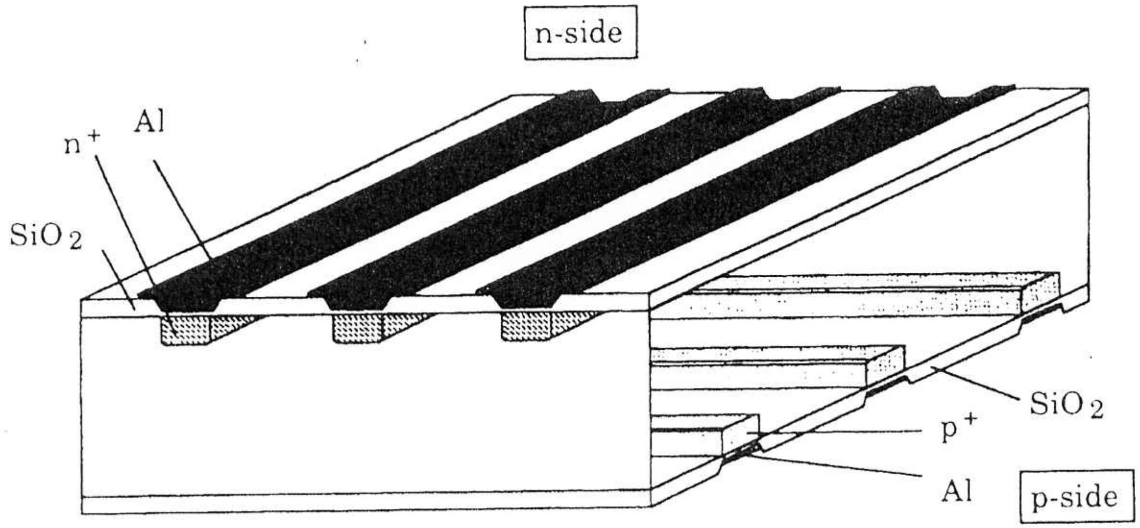

Double-sided silicon strip detector. (From Hubbeling et al.

Space Point

- Harder to fabricate (more expensive)
- Less material – less MCS

Pixel Detector

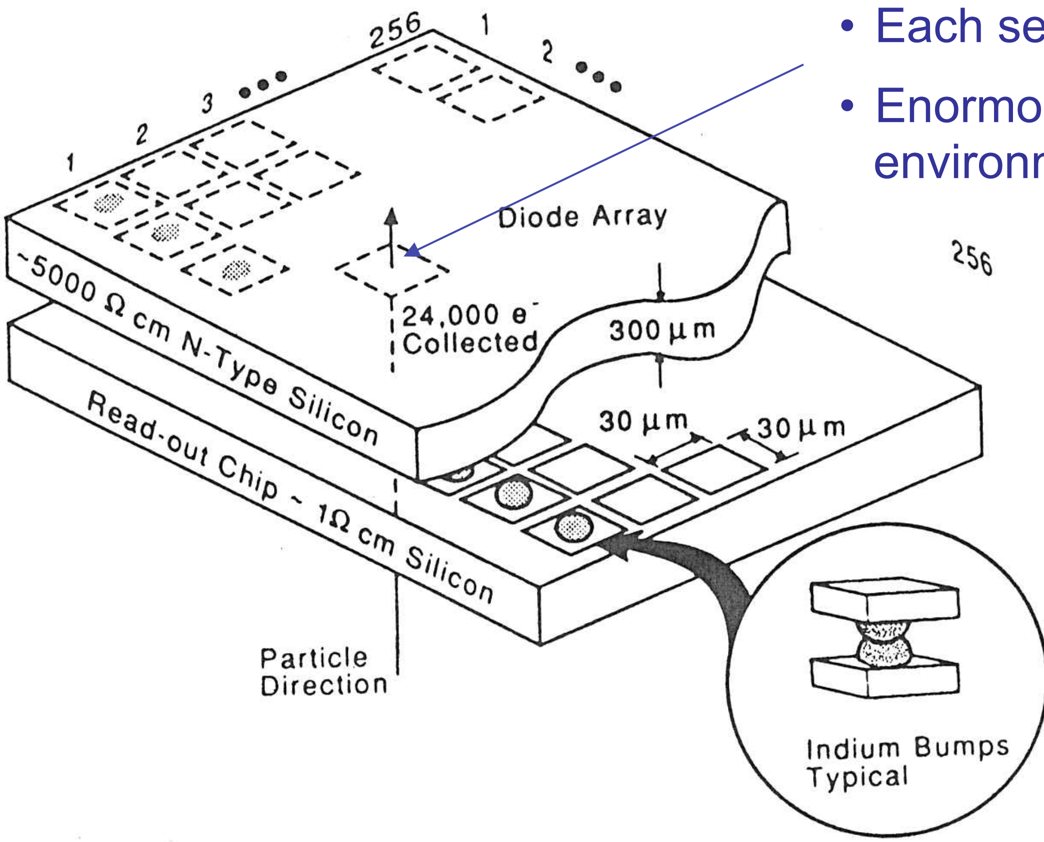

- Each sensor gives a space point
- Enormous advantage in high occupancy environment

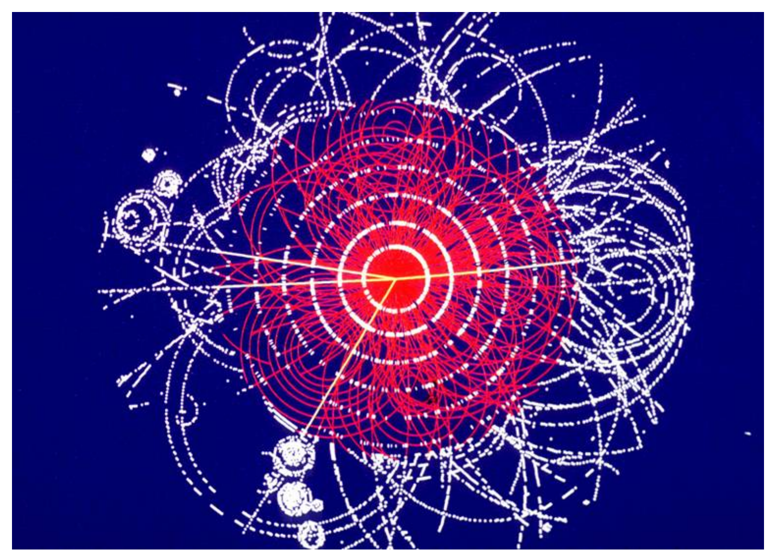

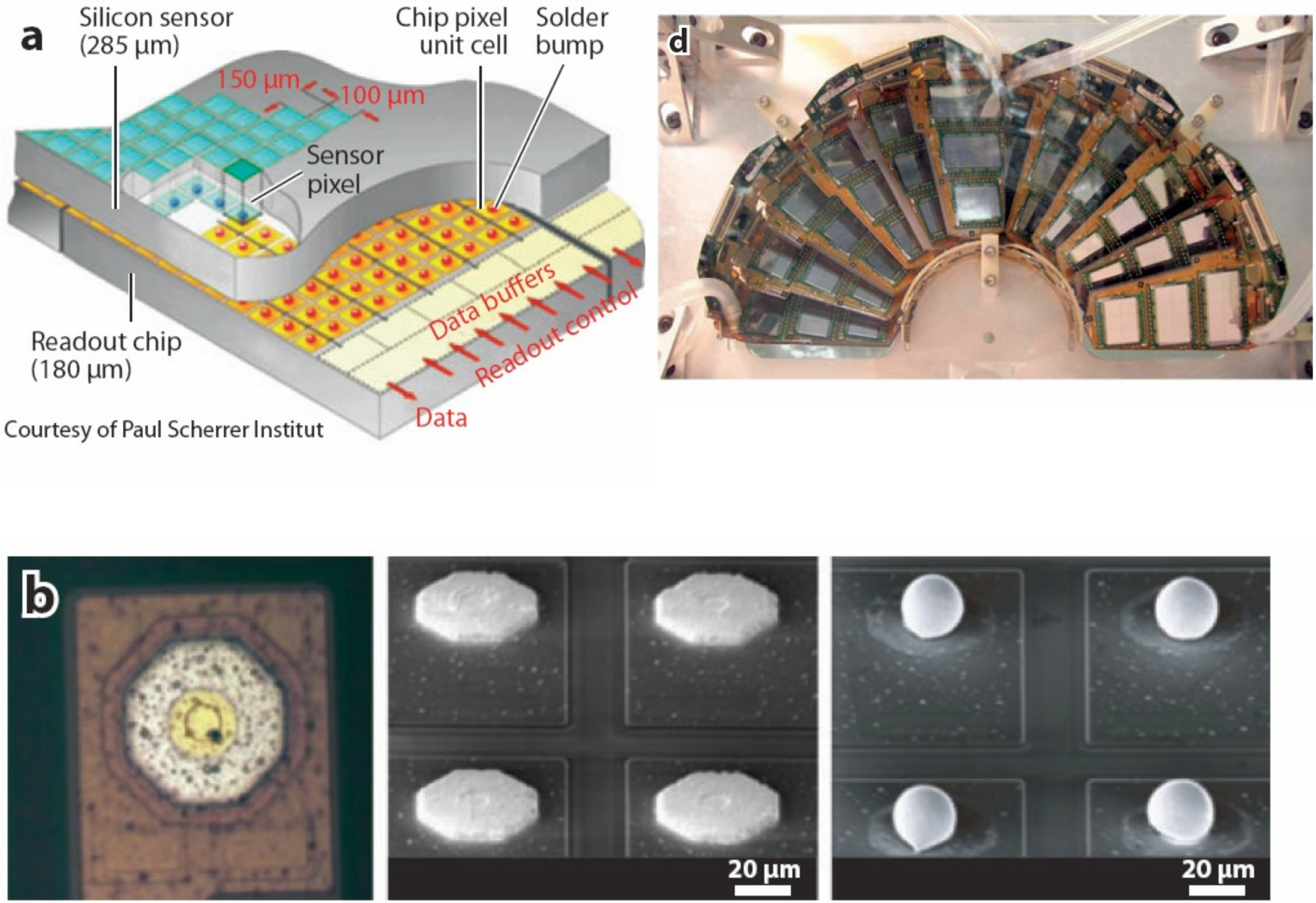
a
Silicon sensor
(285 µm)
150 µm
100 µm
Chip pixel
unit cell
Solder
bump
Sensor
pixel
Readout chip
(180 µm)
Data buffers
Readout control
Data
Courtesy of Paul Scherrer Institut
d
b
20 µm
20 µm

Pixel System

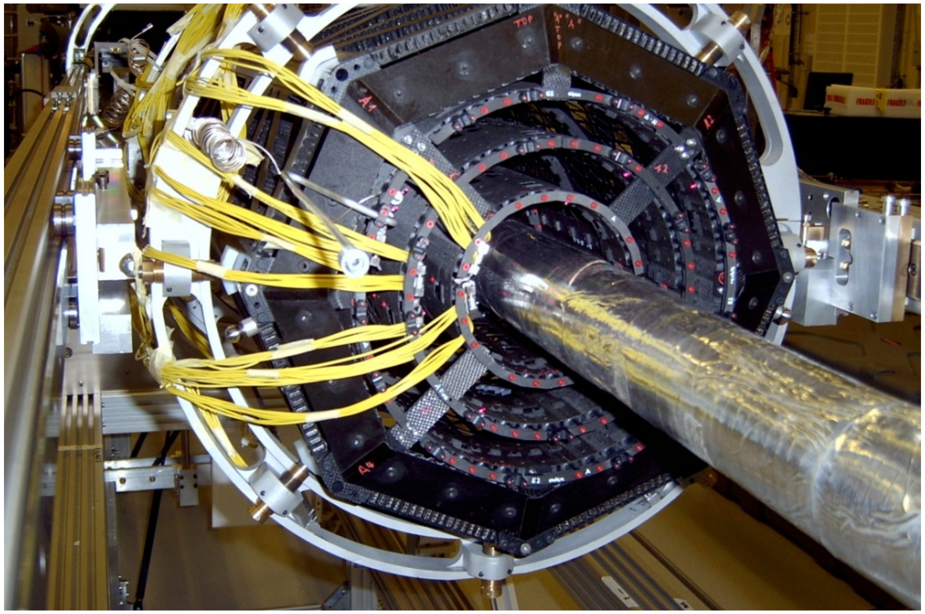

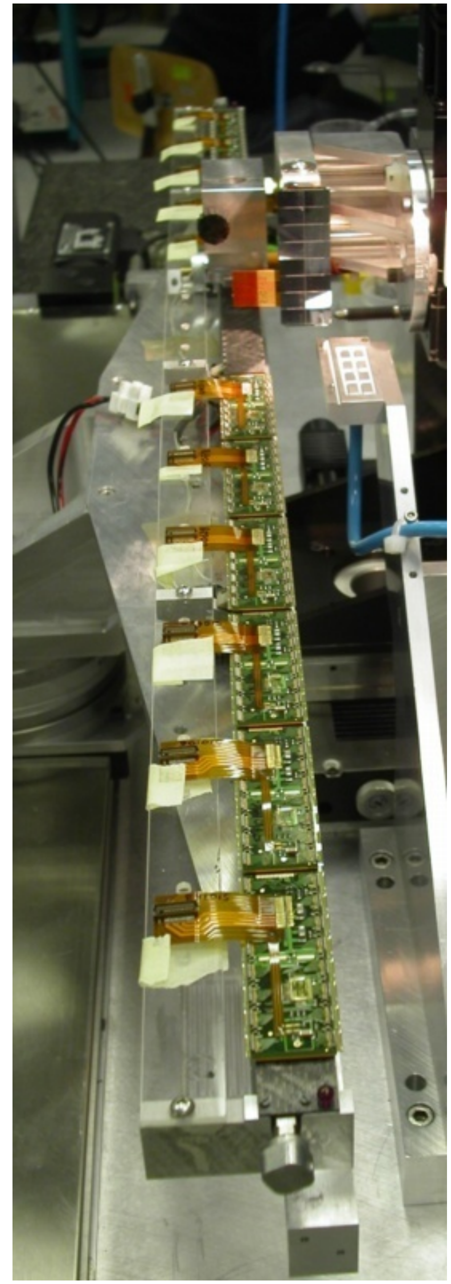

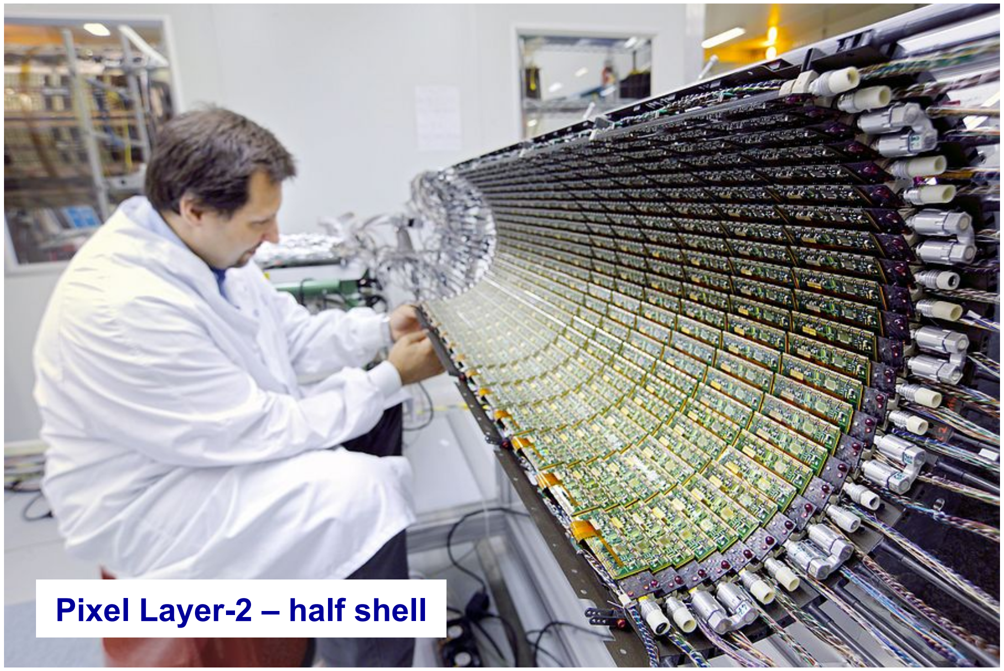

Pixel Layer-2 – half shell

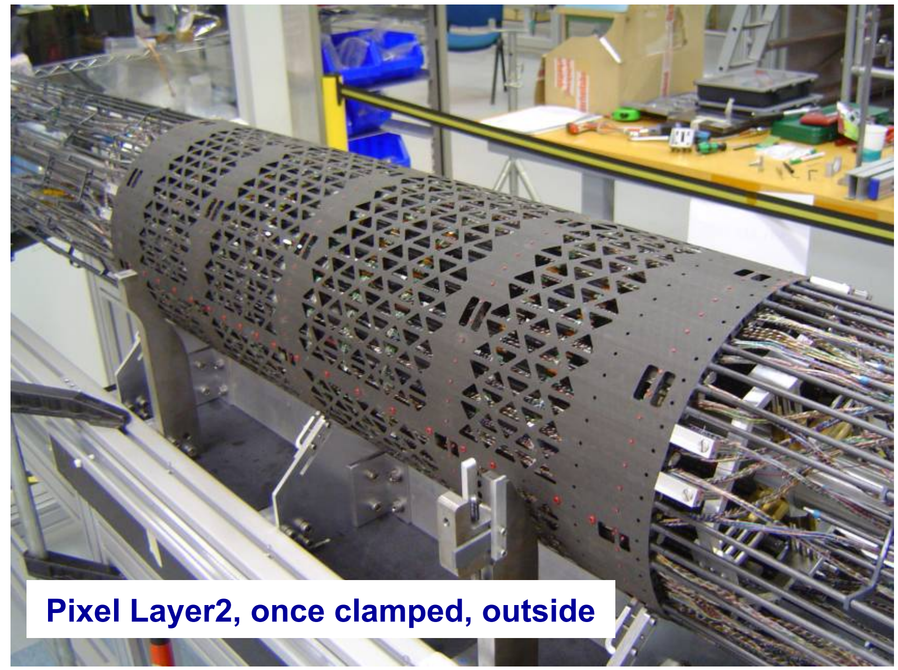

Pixel Layer2, once clamped, outside

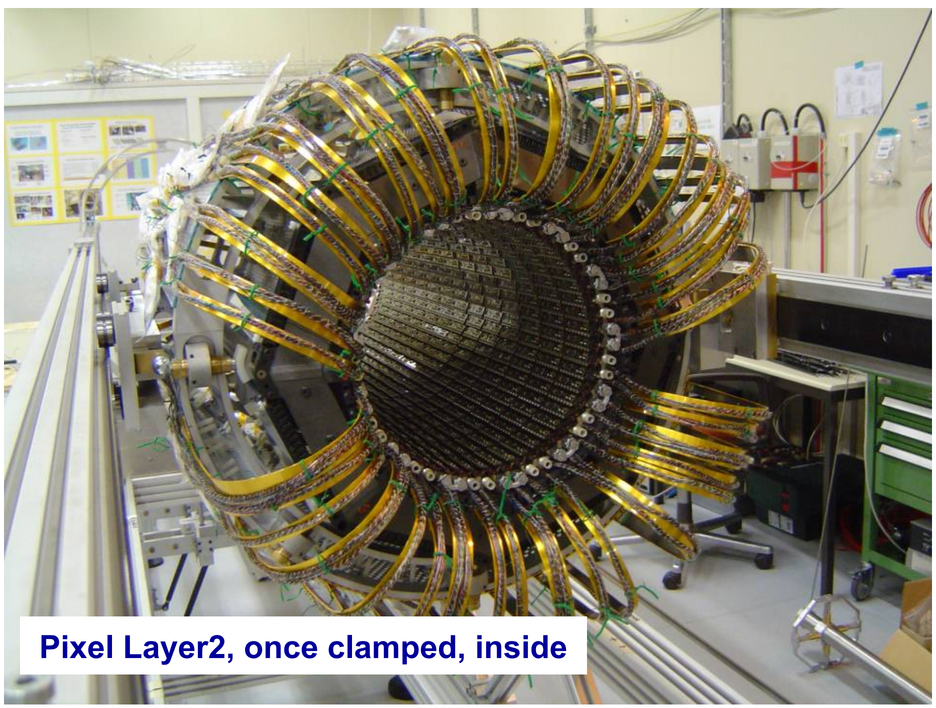

Pixel Layer2, once clamped, inside

"Ready for installation" date is 1st April 2007

Inner Detector (ID)

The Inner Detector (ID) comprises f...
sub-systems:

- Pixels (0.8 10^8 channels)
- Silicon Tracker (SCT) (6 10^6 channels)
- Transition Radiation Tracker (TRT (4 10^5 channels)

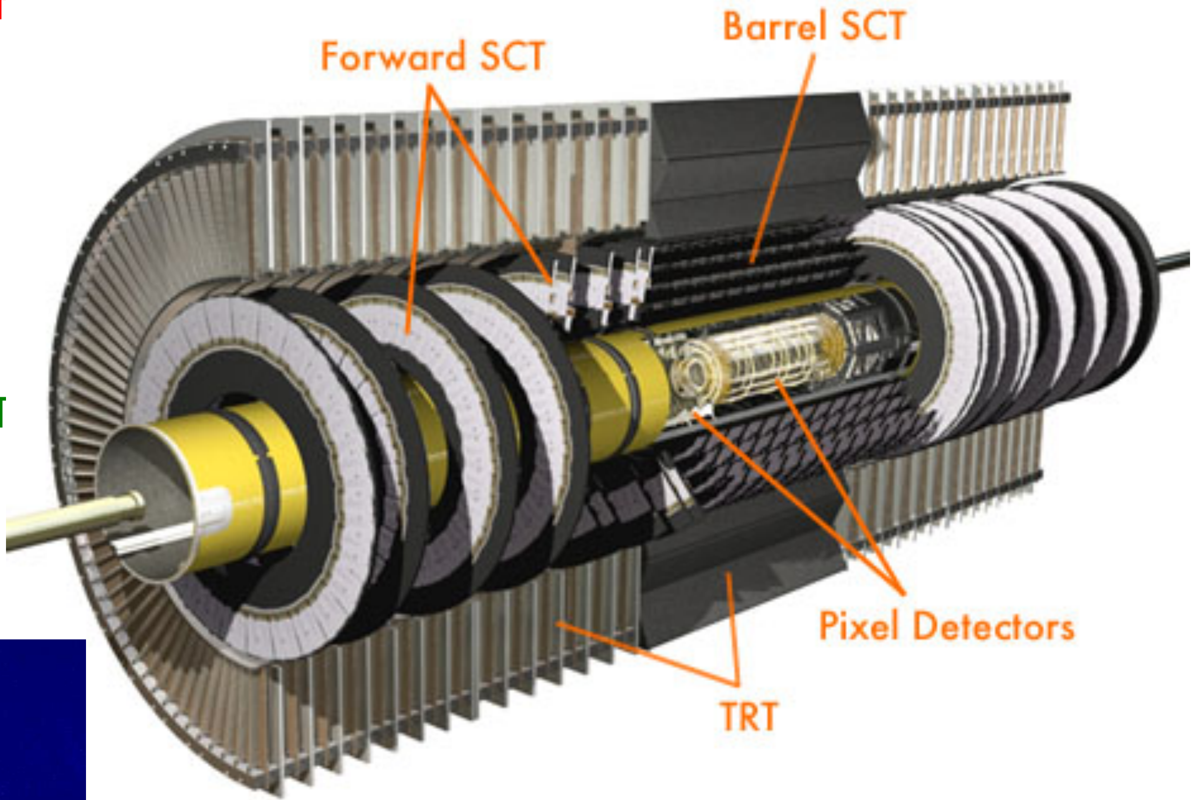

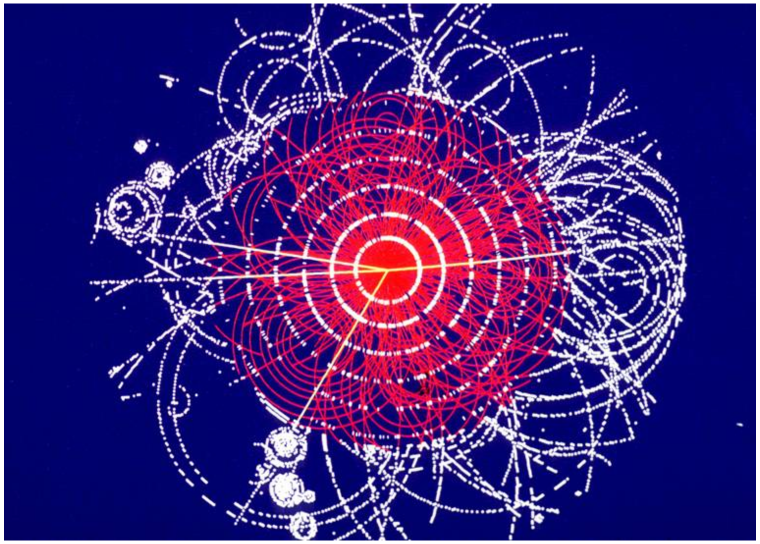

Utility of Si Tracker

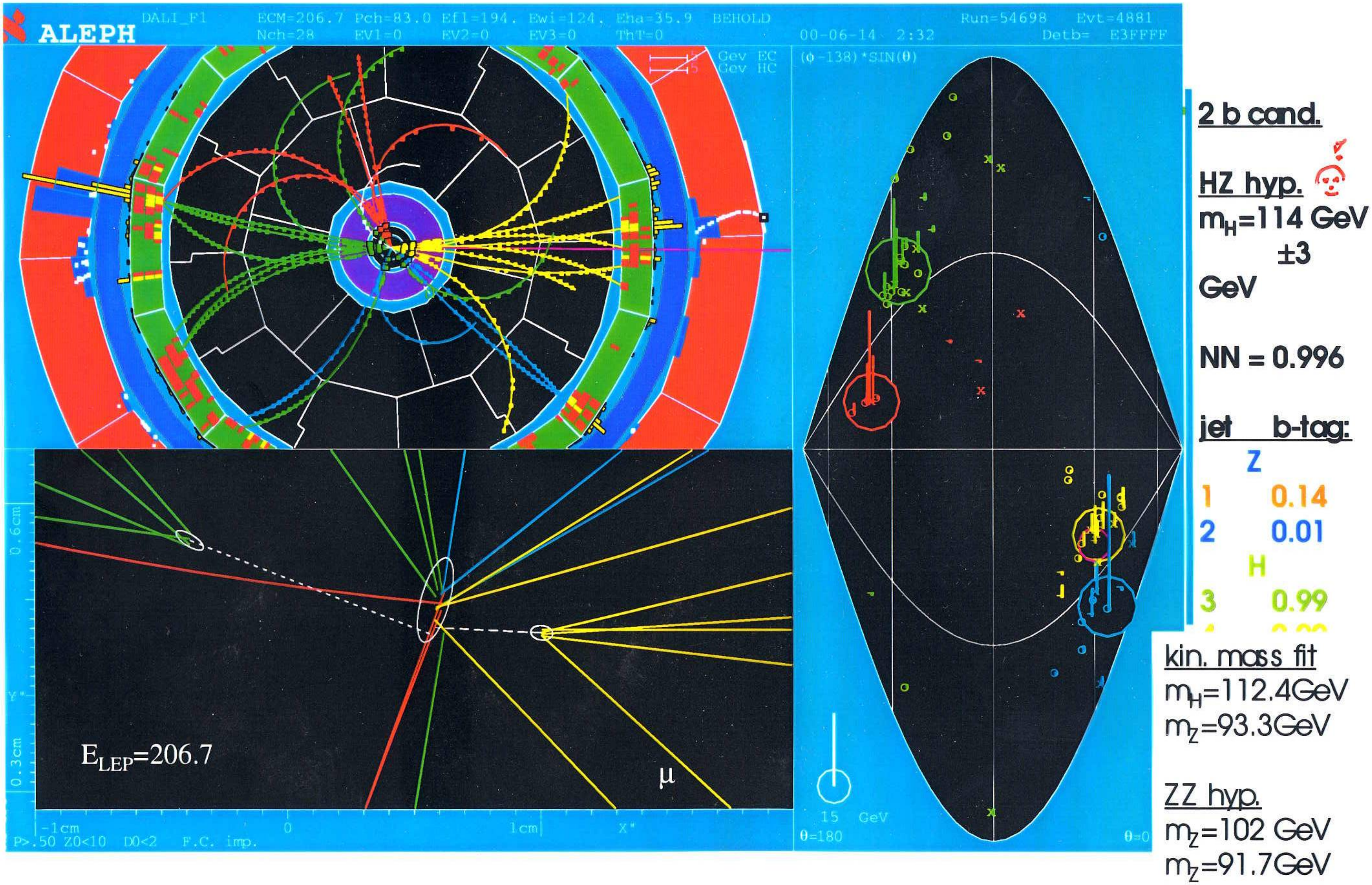

16

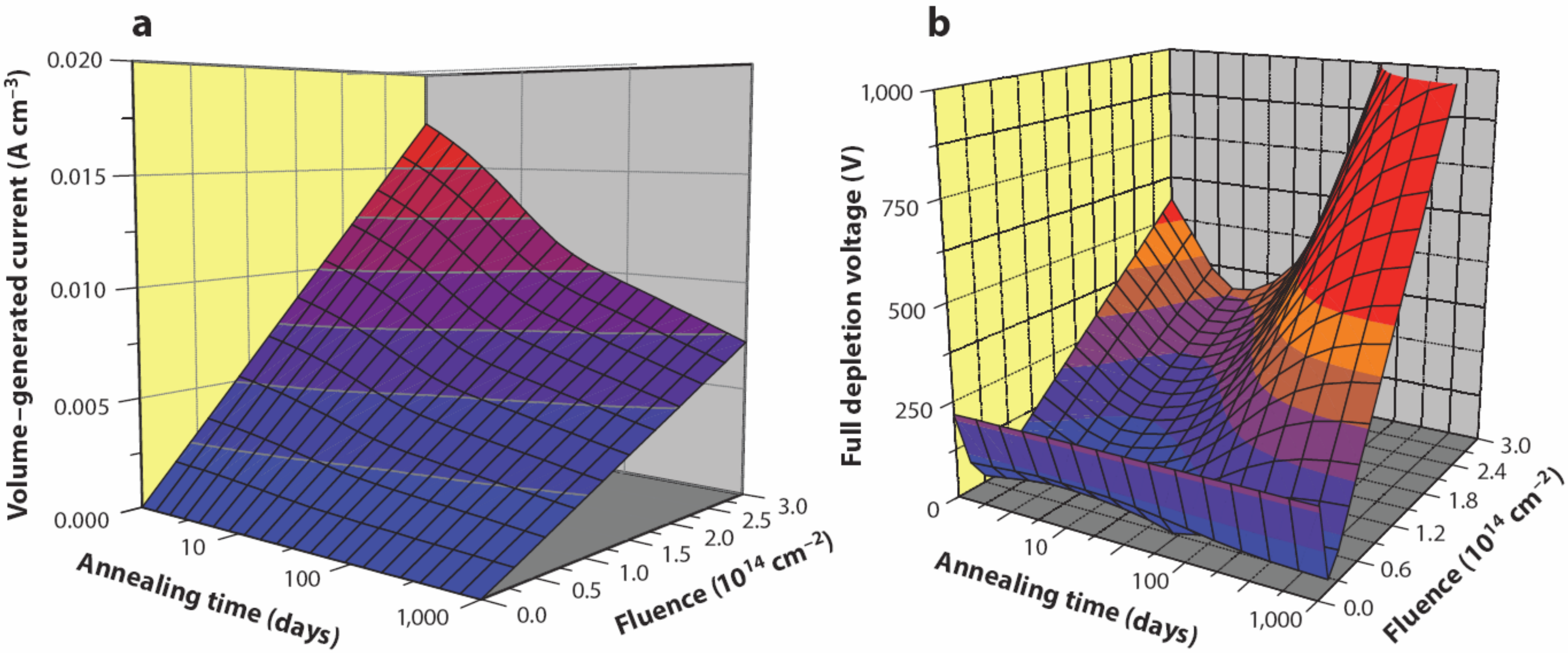

Figure 6

The evolution of current and full depletion voltage ($\sim|N_{\mathrm{eff}}|$) versus fluence and further annealing at room temperature (22). In panel *b*, the dip around 0.5×10^{14} in the fluence axis reveals the space charge sign inversion point; the minimum in the time axis illustrates when the reverse annealing becomes relevant.

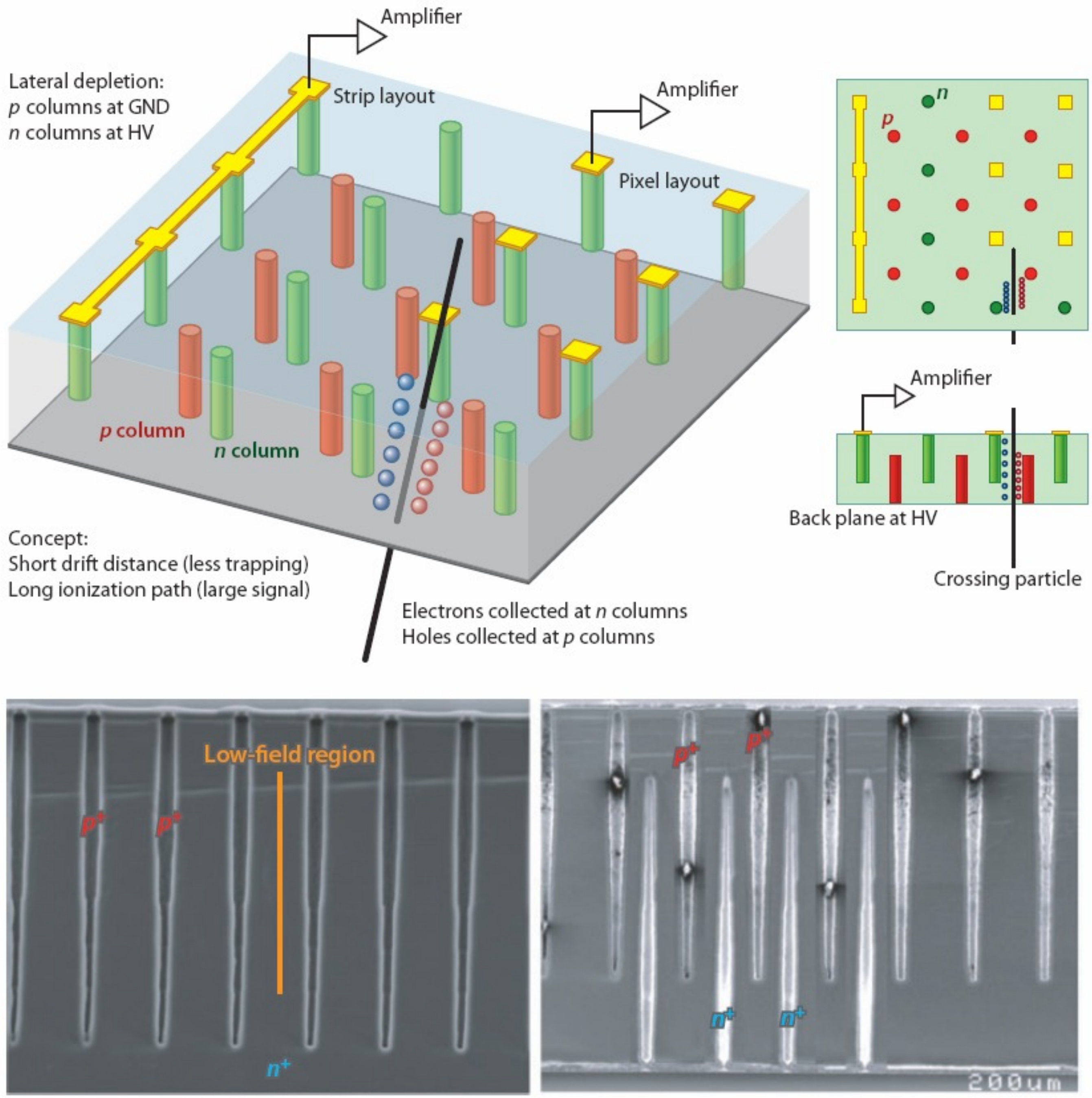

Amplifier
Lateral depletion:
p columns at GND
n columns at HV
Strip layout
Amplifier
Pixel layout
p column
n column
Concept:
Short drift distance (less trapping)
Long ionization path (large signal)
Electrons collected at n columns
Holes collected at p columns
n
p
Amplifier
Back plane at HV
Crossing particle
Low-field region
p+
p+
n+
p+
p+
n+
n+
200um

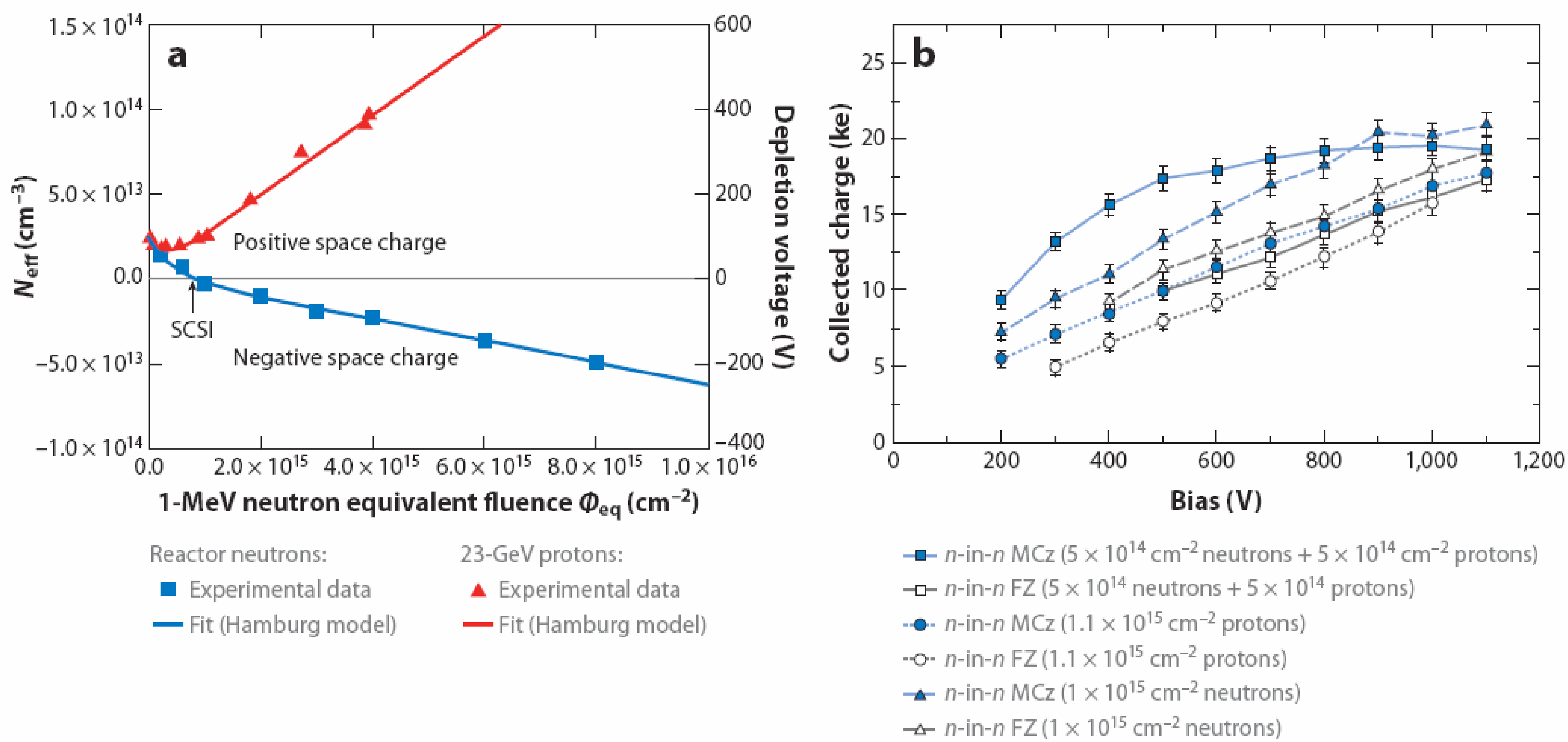
a
1.5 × 10^14
1.0 × 10^14
5.0 × 10^13
0.0
−5.0 × 10^13
−1.0 × 10^14
N_eff (cm^−3)
600
400
200
0
−200
−400
Depletion voltage (V)
Positive space charge
Negative space charge
SCSI
0.0
2.0 × 10^15
4.0 × 10^15
6.0 × 10^15
8.0 × 10^15
1.0 × 10^16
1-MeV neutron equivalent fluence Φ_eq (cm^−2)
Reactor neutrons:
Experimental data
Fit (Hamburg model)
23-GeV protons:
Experimental data
Fit (Hamburg model)
b
0
5
10
15
20
25
Collected charge (ke)
0
200
400
600
800
1,000
1,200
Bias (V)
n-in-n MCz (5 × 10^14 cm^−2 neutrons + 5 × 10^14 cm^−2 protons)
n-in-n FZ (5 × 10^14 neutrons + 5 × 10^14 protons)
n-in-n MCz (1.1 × 10^15 cm^−2 protons)
n-in-n FZ (1.1 × 10^15 cm^−2 protons)
n-in-n MCz (1 × 10^15 cm^−2 neutrons)
n-in-n FZ (1 × 10^15 cm^−2 neutrons)

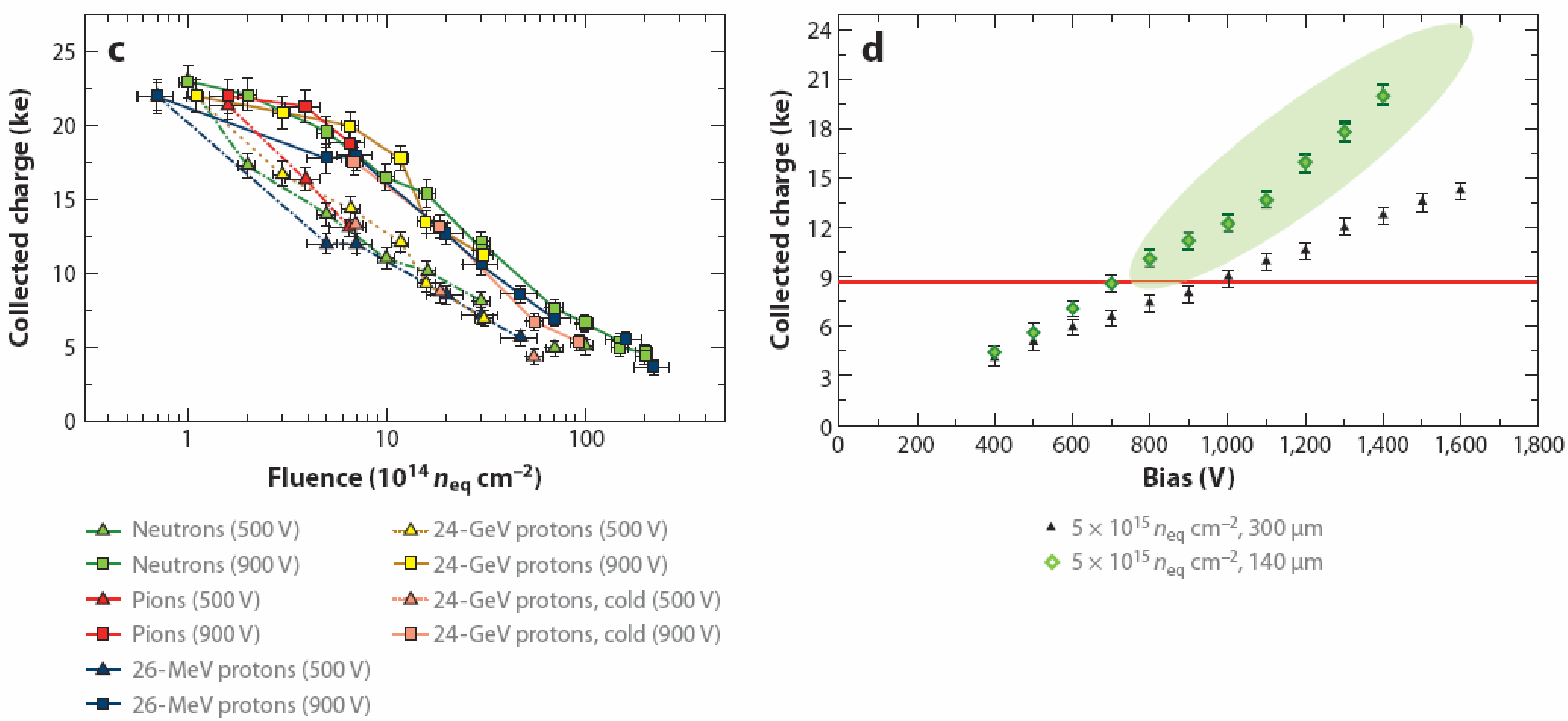
c
Collected charge (ke)
0
5
10
15
20
25
1
10
100
Fluence (10^{14} n_{eq} cm^{-2})
Neutrons (500 V)
Neutrons (900 V)
Pions (500 V)
Pions (900 V)
26-MeV protons (500 V)
26-MeV protons (900 V)
24-GeV protons (500 V)
24-GeV protons (900 V)
24-GeV protons, cold (500 V)
24-GeV protons, cold (900 V)
d
Collected charge (ke)
0
3
6
9
12
15
18
21
24
0
200
400
600
800
1,000
1,200
1,400
1,600
1,800
Bias (V)
5×10^{15} n_{eq} cm^{-2}, 300 μm
5×10^{15} n_{eq} cm^{-2}, 140 μm

Inner Detector Replacement

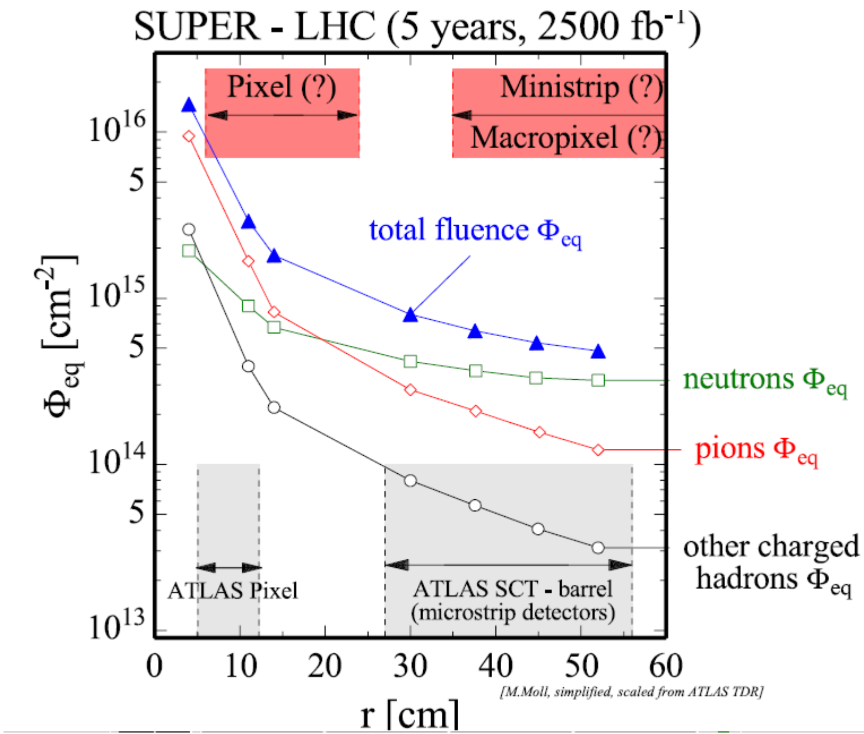

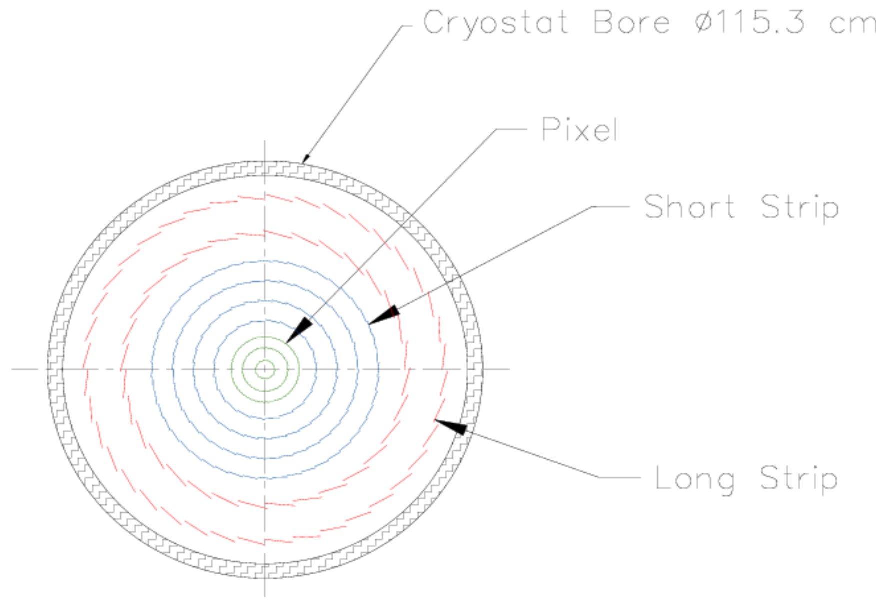

- Order of magnitude increase in Data rates, Occupancy, Irradiation
- No TRT – Si strips
- Pixels moved to larger radius
- New technology for inner layers
- R&D required on sensors, readout, and mechanical engineering

Pixel-layer Technologies

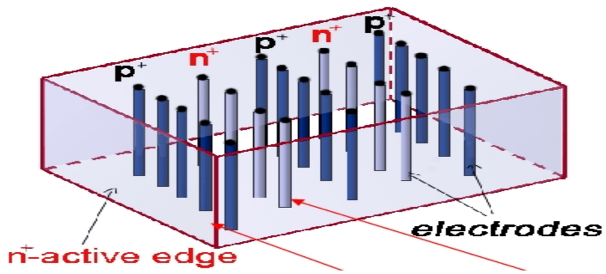

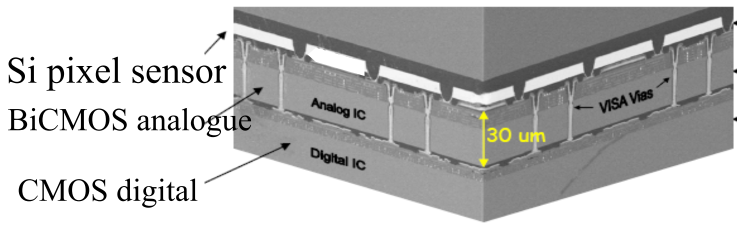

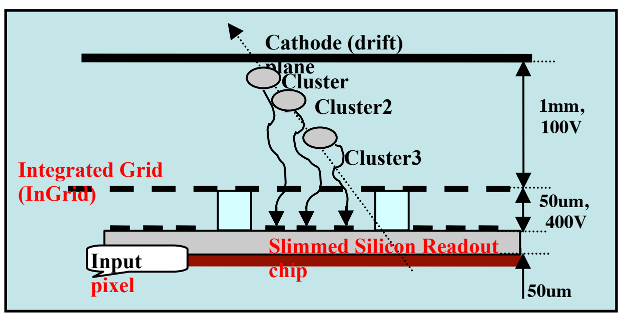

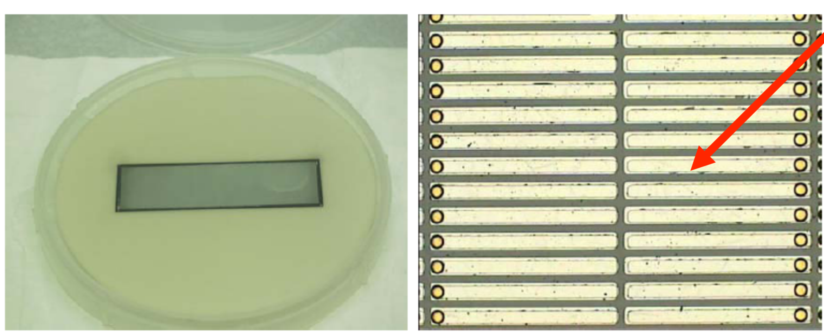

Figure 5: (a) Photograph of the ATLAS pixel diamond mounted in the carrier ready for bump bonding. (b) Zoom view of the pixel pattern after the under-bump metal is deposited.

- Harshest radiation environment (R~4cm)
  - investigate new technologies
- 3D Si
- Thin silicon + 3D interconnects
- Gas over thin pixel (GOSSIP)
- *Diamond pixels*
- May test in pre-SLHC b-layer replacement (~2012)